

Robust Joint Design for Intelligent Reflecting Surfaces Assisted Cell-Free Networks

Xie Xie, Chen He, Xiaoya Li, and Z. Jane Wang, *Fellow, IEEE*

Abstract

Intelligent reflecting surfaces (IRSs) have emerged as a promising economical solution to implement cell-free networks. However, the performance gains achieved by IRSs critically depend on smartly tuned passive beamforming based on the assumption that the accurate channel state information (CSI) knowledge is available at the central processing unit (CPU), which is practically impossible. Thus, in this paper, we investigate the impact of the CSI uncertainty on IRS-assisted cell-free networks. We adopt a stochastic method to cope with the CSI uncertainty by maximizing the expectation of the sum-rate, which guarantees the robust performance over the average. Accordingly, an average sum-rate maximization problem is formulated, which is non-convex and arduous to obtain its optimal solution due to the coupled variables and the expectation operation with respect to CSI uncertainties. As a compromising approach, we develop an efficient robust joint design algorithm with low-complexity. Particularly, the original problem is equivalently transformed into a tractable form by employing algebraic manipulations. Then, the locally optimal solution can be obtained iteratively. **We further prove that the CSI uncertainty has no direct impact on the optimizing of the passive reflecting beamforming.** It is worth noting that the investigated scenario is flexible and general in communications, thus the proposed algorithm can act as a general framework to solve various sum-rate maximization problems. Simulation results demonstrate that IRSs can achieve considerable data rate improvement for conventional cell-free networks, and confirm the resilience of the proposed algorithm against the CSI uncertainty.

Index Terms

Intelligent Reflecting Surface, Cell-Free, Constant Modulus Constraint, Imperfect CSI.

Xie Xie, Chen He, and Xiaoya Li are with the School of Information Science and Technology, Northwest University, Xi'an, 710069, China. Z. Jane Wang is with Department of Electrical and Computer Engineering, The University of British Columbia, Vancouver, BC V6T1Z4, Canada. Corresponding author: Chen He (email: chenhe@nwu.edu.cn).

I. INTRODUCTION

In the past decade, the cell-free networks have been proposed as a promising technology to significantly improve the system performance compared with the traditional multi-cell system [1]. Particularly, cell-free networks advocate a more active treatment of interference, where multiple base-stations (BSs) transmit data to multiple user equipment (UEs) cooperatively and simultaneously. Generally, all BSs are linked to a central processing unit (CPU), where the CPU is responsible for allocating resources of BSs [2]–[4]. However, the performance of cell-free networks are critically depend on the BSs with high hardware-cost and energy-consumption [1].

As a remedy, recently, intelligent reflecting surfaces (IRSs) have attracted a significant amount of attention as a potential economical solution for the future cell-free communication networks [5]. Generally, the basic function of the IRS is to smartly reconfigure the wireless propagation environment by reflecting the incident signal towards the desired spatial direction. Since the IRS composes of a large amount of phase shifters (PSs), each of which operates in a passive way without any decoding and encoding operations, the IRS consumes much less power than the BS [6]. Most importantly, by carefully tuning its passive reflecting beamforming, the IRS can achieve a considerable array performance gain. With these advantages, the IRS has drawn so much interests recently with vast application prospects [7]. The researchers employed the IRS to enhance the performance of communication systems, e.g., improving the data-rate [8]–[11], reducing the transmit power [12], and enhancing energy efficiency [13], etc. Among them, one of the most promising applications was investigated the combining of the IRS and the cell-free network to further enhance the network performance with the low hardware-cost and energy-consumption [14]–[16]. To be specific, the key idea in these works were taking advantage of the IRS to establish a reliable communication link between BSs with UEs, so as to economically implement a virtual cell-free network. Accordingly, the efficient algorithms were provided to joint design the active transmitting beamforming and the passive reflecting beamforming of the BS and the IRS, respectively. Although such works were shown to be effective, they assumed that the high-accuracy full channel state information (CSI) knowledge were perfectly acquired at the BSs (or CPU), which was practically impossible due to the estimation and quantization errors [17]. In fact, the efficient schemes have been extensively studied to estimate CSI knowledge with satisfactory accuracy in IRS-assisted communication systems [18]–[20], however, for the IRS-assisted cell-free networks the estimated CSI were still inaccurate due to that the dimensions

of the channels are large, this makes CSI estimation errors are inevitable [21].

Remarkably, to overcome the impact of the CSI uncertainty on the performance, a few works investigated the robust transmission design for the IRS-assisted communication system that take into account imperfect CSI knowledge. The most contributions in this area assumed a norm-bounded CSI error model, which is commonly employed when the CSI error is dominated by quantization errors [22]. Under this error model, the authors in [23]–[25] proposed the min-max (worst-case) constrained robust design schemes to fight against the CSI uncertainty. In general, the channel estimation error is modelled as a random variable which follows a known probability distribution (e.g., Gaussian distribution), and which is unbounded [22], [26], [27]. As a result, an statistical CSI error model was applicable to characterize the practical imperfect CSI mainly due to the channel estimation errors [17]. The robustness under this error model were provided by solving the outage probability constrained problem or using the expected/averaged performance [17], [22], [27]. The robust designs for IRS-assisted MISO communication system subjected to the rate outage probability constraints have been reported in [17], [27]–[29]. The authors in [30] and [31] proposed a pair of novel robust beamforming design schemes for the IRS-assisted MISO system, to minimize the mean squared error and to maximize the average sum-rate, respectively. It would like to mentioned that the above works [30], [31] adopted the stochastic method to address the CSI uncertainties by using the expected or the averaged performance, though it does not ensure the robust performance for each individual realization [22], [26].

Motivated by the discussions as mentioned above, in this paper, we investigate the robust joint design in the IRS assisted cell-free MIMO communication network, where the statistical CSI error model of all channels are assumed. we adopt the stochastic method [22], [26] to cope with the CSI uncertainty by maximizing the expectation of the sum-rate, which guaranteed the robust performance over the average. Accordingly, our goal is to maximize the average sum-rate by joint designing the active transmitting beamforming and the passive reflecting beamforming of the BSs and the IRSs, respectively, while satisfying the power constraint at per BS and the constant modulus constraint at per PS of IRSs.

The main contributions of this paper are summarized as follows

- To our best knowledge, this is the first work to study the robust joint design of IRS-assisted cell-free MIMO networks in the presence of imperfect CSI knowledge. It is worthy pointing out that the considered scenario is very flexible and general in wireless communication systems, i.e., multiple BSs and UEs with multiple transmitting and receiving antennas,

multiple IRSs with multiple PSs, and all the channels are imperfect, hence, most existing works that focus on maximizing sum-rate under both the perfect CSI or the statistical CSI error, are special cases of this paper. Thus, the proposed algorithm can act as a general framework to solve various sum-rate maximization problem in both the IRS-assisted or the conventional without-IRS wireless communication systems;

- The formulated problem is challenging to solve due to the non-convex objective function, the intricately coupled variables, the constant modulus constraints, and the expectation operator about the uncertainty terms. As a compromising approach, we first transform the original non-convex problem to an equivalent but tractable form by extending the fractional programming method, e.g., quadratic transform (QT) and Lagrangian dual transform (LDT) into matrix-forms. Then, the transformed problem is decomposed into two subproblems, i.e., the active transmit beamforming matrices optimization and the passive reflecting beamforming matrices optimization. Next, the two subproblems can be solved alternating iteratively by employing the Lagrangian dual multiplier method and alternate sequential optimization (ASO) algorithm with the locally optimal solutions in nearly closed-forms, respectively;
- Moreover, after employing algebraic manipulations, we proof that the expectation value with respect to the CSI uncertainty has no direct impact on the optimizing of the passive reflecting beamforming;
- Simulation results demonstrate that IRSs can significantly improve the data-rate, and confirm that the proposed robust joint design has the resilience against imperfect CSI knowledge.

Notations: Vectors and matrices are presented by bold-face lower-case and upper-case letters, respectively. $\mathcal{CN}(0, \mathbf{I})$ denotes the circularly symmetric complex Gaussian (CSCG) distribution with zero mean and covariance matrix $\mathbf{I}_{\mathcal{N}}$, where $\mathbf{I}_{\mathcal{N}}$ denotes $\mathcal{N} \times \mathcal{N}$ identity matrix. $\mathbb{E}\{\cdot\}$ denotes the expectation operator. $\text{Vec}\{\cdot\}$ stacks all the columns of the argument into a single column vector and $\text{Vecd}\{\cdot\}$ forms a vector out of the diagonal of its matrix argument. \otimes and \odot denote the Kronecker and the Hadamard products, respectively. \mathbf{A}^H and $\text{Tr}(\mathbf{A})$ denote the Hermitian and trace operators of the matrix \mathbf{A} , respectively. $\text{Re}\{a\}$ is the real part of a .

II. NETWORK MODEL AND PROBLEM FORMULATION

As shown in Fig. 1, we describe a distributed multiple IRSs assisted cell-free MIMO downlink communication system [32], where \mathcal{L} distributed BSs and \mathcal{R} distributed IRSs are linked to a CPU and serve \mathcal{K} UEs cooperatively, where the CPU is responsible for optimizing both the active and

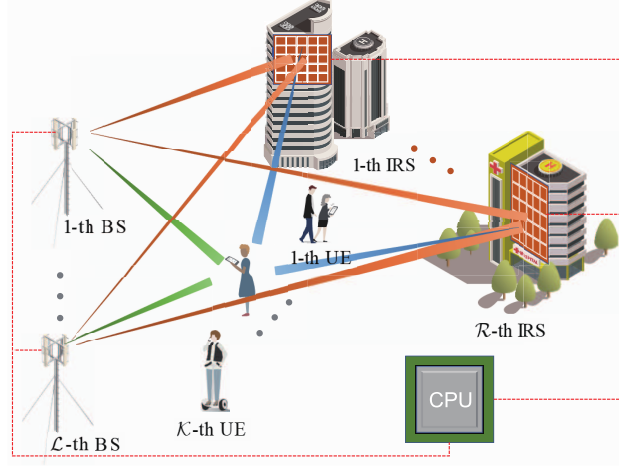


Fig. 1. IRSs-assisted cell-free MIMO system model.

passive beamforming matrices and then the BSs and the IRSs exploit the beamforming matrices to precode and reconfigure the signals. Moreover, each BS, IRS, and UE are equipped with \mathcal{M}_B transmitting antennas, \mathcal{N} PSs, and \mathcal{M}_U receiving antennas, respectively. The signals reflected by the IRS two or more times are ignored.

A. Channel Model

We assume a narrow-band system and let $\mathbf{D}_{l,k} \in \mathbb{C}^{\mathcal{M}_B \times \mathcal{M}_U}$ denotes the direct channel from the l -th BS to the k -th UE, and $\mathbf{G}_{r,k} \in \mathbb{C}^{\mathcal{N} \times \mathcal{M}_U}$ is the channel from the r -th IRS to the k -th UE. The channel from the l -th BS to the r -th IRS is represented by $\mathbf{S}_{l,r} \in \mathbb{C}^{\mathcal{N} \times \mathcal{M}_B}$. We assume the small-scale fading of the direct channels (i.e., $\mathbf{D}_{l,k}, \forall l, k$) and the IRS-related channels (i.e., $\mathbf{G}_{r,k}, \forall r, k$ and $\mathbf{S}_{l,r}, \forall l, r$) are Rayleigh fading and Rician fading [10], respectively. Besides, we further assume that the BSs and the UEs are equipped with uniform linear arrays (ULAs), and the IRSs are modeled as uniform planar arrays (UPAs) [14], [33], [34].

With the IRSs, the transmitted signal can be dynamically altered by its \mathcal{N} PSs, where the diagonal passive reflecting beamforming matrices are denoted as

$$\mathbf{\Theta}_r = \alpha \text{diag} (e^{j\phi_{r,1}}, e^{j\phi_{r,2}}, \dots, e^{j\phi_{r,\mathcal{N}}}) \in \mathbb{C}^{\mathcal{N} \times \mathcal{N}}, \forall r \in \mathcal{R}, \quad (1)$$

where $\alpha \in [0, 1]$ denotes the reflecting efficiency of IRSs, which is used to measure the power loss caused by the signal absorption of the IRS, and $\phi_{r,n} \in [0, 2\pi)$ is the phase-shifting of the n -th PS of the r -th IRS.

In general, to acquire the CSI knowledge with satisfactory accuracy is challenging to realize in IRS-assisted cell-free networks, thus, to account for the estimation error of the acquired CSI knowledge, we consider CSI knowledge of both the direct and the IRS-related channels uncertain. Let $\mathbf{H}_{l,k} \in \mathbb{C}^{\mathcal{M}_B \times \mathcal{M}_U}$ denotes the equivalent actual channel spanning from the l -th BS to the k -th UE, which can be modeled as

$$\mathbf{H}_{l,k}^H = \hat{\mathbf{D}}_{l,k}^H + \bar{\mathbf{D}}_{l,k}^H + \sum_{r=1}^{\mathcal{R}} \left(\hat{\mathbf{G}}_{r,k}^H + \bar{\mathbf{G}}_{r,k}^H \right) \boldsymbol{\Theta}_r \left(\hat{\mathbf{S}}_{l,r} + \bar{\mathbf{S}}_{l,r} \right), \forall l, k, \quad (2)$$

where $\hat{\mathbf{D}}_{l,k}$, $\hat{\mathbf{G}}_{r,k}$, and $\hat{\mathbf{S}}_{l,r}$ are estimated CSI by using efficient estimation schemes for IRS-assisted systems [18]–[20], [35], and $\bar{\mathbf{D}}_{l,k}$, $\bar{\mathbf{G}}_{r,k}$, and $\bar{\mathbf{S}}_{l,r}$ are the additive CSI estimation errors. As [17], [27]–[31], we assume the statistical CSI error model, which is applicable when the error is predominantly due to unavoidable inaccurate channel estimation in practical scenarios [27]. Thus, the CSI error matrices $\bar{\mathbf{D}}_{l,k}$, $\bar{\mathbf{G}}_{r,k}$, and $\bar{\mathbf{S}}_{l,r}$ are assumed to follow the Gaussian distribution [17], [22] with zero mean and

$$\mathbb{E} \left\{ \text{Vec}(\bar{\mathbf{D}}_{l,k}) \text{Vec}(\bar{\mathbf{D}}_{l,k})^H \right\} = \delta_{\mathbf{D}_{l,k}}^2 \mathbf{I}_{\mathcal{M}_B \mathcal{M}_U}, \forall l, k, \quad (3a)$$

$$\mathbb{E} \left\{ \text{Vec}(\bar{\mathbf{G}}_{r,k}) \text{Vec}(\bar{\mathbf{G}}_{r,k})^H \right\} = \delta_{\mathbf{G}_{r,k}}^2 \mathbf{I}_{\mathcal{N} \mathcal{M}_U}, \forall r, k, \quad (3b)$$

$$\mathbb{E} \left\{ \text{Vec}(\bar{\mathbf{S}}_{l,r}) \text{Vec}(\bar{\mathbf{S}}_{l,r})^H \right\} = \delta_{\mathbf{S}_{l,r}}^2 \mathbf{I}_{\mathcal{N} \mathcal{M}_B}, \forall l, r, \quad (3c)$$

where $\delta_{\mathbf{D}_{l,k}}^2 = \kappa_{\mathbf{D}}^2 \left\| \text{Vec}(\hat{\mathbf{D}}_{l,k}) \right\|_2^2$, $\delta_{\mathbf{G}_{r,k}}^2 = \kappa_{\mathbf{G}}^2 \left\| \text{Vec}(\hat{\mathbf{G}}_{r,k}) \right\|_2^2$, and $\delta_{\mathbf{S}_{l,r}}^2 = \kappa_{\mathbf{S}}^2 \left\| \text{Vec}(\hat{\mathbf{S}}_{l,r}) \right\|_2^2$, with $\kappa_{\mathbf{D}/\mathbf{G}/\mathbf{S}}^2 \in [0, 1)$ are normalized CSI errors, which are used to measure the relative amount of the CSI uncertainties. Further, all the CSI error covariances are assumed to be known at the CPU [22].

By defining $\boldsymbol{\Theta} = \text{blkdiag} \{ \boldsymbol{\Theta}_1, \boldsymbol{\Theta}_2, \dots, \boldsymbol{\Theta}_{\mathcal{R}} \} \in \mathbb{C}^{\mathcal{R} \mathcal{N} \times \mathcal{R} \mathcal{N}}$, $\mathbf{G}_k = [\mathbf{G}_{1,k}^T, \mathbf{G}_{2,k}^T, \dots, \mathbf{G}_{\mathcal{R},k}^T]^T \in \mathbb{C}^{\mathcal{R} \mathcal{N} \times \mathcal{M}_U}$, $\mathbf{S}_l = [\mathbf{S}_{l,1}^T, \mathbf{S}_{l,2}^T, \dots, \mathbf{S}_{l,\mathcal{R}}^T]^T \in \mathbb{C}^{\mathcal{R} \mathcal{N} \times \mathcal{M}_B}$, we have

$$\mathbf{H}_{l,k}^H \triangleq \hat{\mathbf{H}}_{l,k}^H + \bar{\mathbf{H}}_{l,k}^H, \forall l, k, \quad (4)$$

where $\hat{\mathbf{H}}_{l,k}^H \triangleq \hat{\mathbf{D}}_{l,k}^H + \hat{\mathbf{G}}_k^H \boldsymbol{\Theta} \hat{\mathbf{S}}_l^H$ and $\bar{\mathbf{H}}_{l,k}^H \triangleq \bar{\mathbf{D}}_{l,k}^H + \bar{\mathbf{G}}_k^H \boldsymbol{\Theta} \bar{\mathbf{S}}_l^H + \hat{\mathbf{G}}_k^H \boldsymbol{\Theta} \bar{\mathbf{S}}_l^H + \bar{\mathbf{G}}_k^H \boldsymbol{\Theta} \hat{\mathbf{S}}_l^H$.

B. Network Model

The signal transmitted from the \mathcal{L} BSs can be mathematically expressed as

$$\mathbf{x} = \sum_{l=1}^{\mathcal{L}} \sum_{k=1}^{\mathcal{K}} \mathbf{W}_{l,k} \mathbf{s}_{l,k}, \forall l \in \mathcal{L}, \forall k \in \mathcal{K}. \quad (5)$$

where $\mathbf{s}_{l,k} \in \mathbb{C}^{d \times 1}$ denotes d desired data streams from the l -th BS intend for the k -th UE and satisfies $\mathbf{s}_{l,k} \sim \mathcal{CN}(\mathbf{0}, \mathbf{I}_d)$. $\mathbf{W}_{l,k} \in \mathbb{C}^{\mathcal{M}_B \times d}$ is the corresponding active transmitting beamforming matrix from the l -th BS to the k -th UE, the transmit power at each BS is $\sum_{k=1}^{\mathcal{K}} \mathbb{E} \{ \mathbf{s}_{l,k}^H \mathbf{W}_{l,k}^H \mathbf{W}_{l,k} \mathbf{s}_{l,k} \} = \sum_{k=1}^{\mathcal{K}} \|\mathbf{W}_{l,k}\|_F^2$.

The received signal at the k -th UE can be expressed by

$$\mathbf{y}_k = \sum_{l=1}^{\mathcal{L}} \hat{\mathbf{H}}_{l,k}^H \mathbf{W}_{l,k} \mathbf{s}_{l,k} + \sum_{l=1}^{\mathcal{L}} \sum_{\substack{i=1 \\ i \neq k}}^{\mathcal{K}} \hat{\mathbf{H}}_{l,k}^H \mathbf{W}_{l,i} \mathbf{s}_{l,i} + \sum_{l=1}^{\mathcal{L}} \sum_{i=1}^{\mathcal{K}} \bar{\mathbf{H}}_{l,k}^H \mathbf{W}_{l,i} \mathbf{s}_{l,i} + \mathbf{n}_k, \quad (6)$$

where $\mathbf{n}_k \sim \mathcal{CN}(\mathbf{0}, \sigma_k^2 \mathbf{I}_{\mathcal{M}_U})$ is the background additive white Gaussian noise (AWGN) vector at the k -th UE.

Based on the aforementioned discussions, the signal to interference plus noise ratio (SINR) matrix at the k -th UE can be formulated as

$$\Gamma_k = \sum_{l=1}^{\mathcal{L}} \hat{\mathbf{H}}_{l,k}^H \mathbf{W}_{l,k} \mathbf{V}_k^{-1} \mathbf{W}_{l,k}^H \hat{\mathbf{H}}_{l,k}, \quad \forall k \in \mathcal{K}, \quad (7)$$

where \mathbf{V}_k denotes the covariance of the effective interference plus noise and is calculated as

$$\mathbf{V}_k = \sum_{l=1}^{\mathcal{L}} \sum_{\substack{i=1 \\ i \neq k}}^{\mathcal{K}} \hat{\mathbf{H}}_{l,k}^H \mathbf{W}_{l,i} \mathbf{W}_{l,i}^H \hat{\mathbf{H}}_{l,k} + \sum_{l=1}^{\mathcal{L}} \sum_{i=1}^{\mathcal{K}} \bar{\mathbf{H}}_{l,k}^H \mathbf{W}_{l,i} \mathbf{W}_{l,i}^H \bar{\mathbf{H}}_{l,k} + \sigma_k^2 \mathbf{I}_{\mathcal{M}_U}. \quad (8)$$

We adopt a stochastic method to address the CSI uncertainties by maximizing the expectation of the sum-rate that depend on the CSI error. Such stochastic method guarantees the robust performance over the average, though it does not ensure the robust performance for each individual realization [22]. By collecting all the active transmit beamforming matrices at \mathcal{L} BSs as $\tilde{\mathbf{W}} = \{\mathbf{W}_{l,k}, \forall l, k\}$ and the passive reflecting beamforming matrices at \mathcal{R} IRSs as $\tilde{\Theta} = \{\Theta_r, \forall r\}$, the average sum-rate of the IRS-assisted cell-free network is given by

$$\mathcal{R}(\tilde{\mathbf{W}}, \tilde{\Theta}) = \mathbb{E} \left\{ \sum_{k=1}^{\mathcal{K}} \log |\mathbf{I}_{\mathcal{M}_U} + \Gamma_k| \right\}, \quad (9)$$

where the expectation is taken over all uncertain terms, i.e., the unknown CSI estimation error matrices $\bar{\mathbf{D}}_{l,k}$, $\bar{\mathbf{G}}_{r,k}$, and $\bar{\mathbf{S}}_{l,r}, \forall l, r, k$, which is main challenge to solve this problem.

C. Problem Formulation

In this paper, our objective is maximizing the average sum-rate through joint optimizing the robust active transmit beamforming $\tilde{\mathbf{W}}$ and the robust passive reflecting beamforming $\tilde{\Theta}$ with the imperfect CSI knowledge, while satisfying the power constraint of per BS and the constant

modulus constraint of per PS. Accordingly, the average sum-rate of the IRS-assisted cell-free network maximization problem can be mathematically formulated as

$$\mathcal{P}_1 : \max_{\tilde{\mathbf{W}}, \tilde{\Theta}} \mathcal{R}(\tilde{\mathbf{W}}, \tilde{\Theta}) \quad (10a)$$

$$\text{s. t.} \quad \sum_{k=1}^{\mathcal{K}} \|\mathbf{W}_{l,k}\|_{\text{F}}^2 \leq P_l^{\max}, \forall l \in \mathcal{L}, \quad (10b)$$

$$|\Theta_{n,n}| = \alpha, \forall n \in \mathcal{RN}, \quad (10c)$$

where the constraint (10b) limits the maximum transmit power of each BS and (10c) represents the constant modulus constraint of each PS at the IRSs. Due to the optimizing variables are intricately coupled in the matrix-ratio terms, the problem \mathcal{P}_1 is non-convex and arduous to tackle by employing the existing methods directly. Besides, the expectation operator with respect to uncertain terms, i.e., CSI estimation errors, makes the formulated problem becomes rather challenging. Thus, in the following section, we provide a robust joint design algorithm to solve the above non-convex problem.

III. PROPOSED ROBUST JOINT DESIGN ALGORITHM

In this section, we describe the proposed robust joint design of the active transmitting beamforming of BSs and the passive reflecting beamforming of IRS with the CSI uncertainties.

As a compromising approach, we consider to transform the intractable problem \mathcal{P}_1 into an equivalent form by extending the well-known fractional programming (FP) methods, e.g., quadratic transform (QT) [36, Corollary 1] and Lagrangian dual transform (LDT) [36, Theorem 4] into matrix-forms. Accordingly, we have the following proposition:

Proposition 1. *By introducing a pair of auxiliary matrices $\tilde{\mathbf{U}} = \{\mathbf{U}_k \in \mathbb{C}^{d \times d}, \forall k\}$ and $\tilde{\mathbf{Y}} = \{\mathbf{Y}_k \in \mathbb{C}^{\mathcal{M}_U \times d}, \forall k\}$, the formulated problem \mathcal{P}_1 can be equivalently transformed as*

$$\mathcal{P}_2 : \max_{\tilde{\mathbf{W}}, \tilde{\Theta}, \tilde{\mathbf{U}}, \tilde{\mathbf{Y}}} f_1(\tilde{\mathbf{W}}, \tilde{\Theta}, \tilde{\mathbf{U}}, \tilde{\mathbf{Y}}) \quad (11a)$$

$$\text{s. t.} \quad (10b), (10c), \quad (11b)$$

where the objective function is given by

$$\begin{aligned}
f_1(\tilde{\mathbf{W}}, \tilde{\mathbf{\Theta}}, \tilde{\mathbf{U}}, \tilde{\mathbf{Y}}) &= \sum_{k=1}^{\mathcal{K}} \log |\bar{\mathbf{U}}_k| - \sum_{k=1}^{\mathcal{K}} \text{Tr}(\mathbf{U}_k) + \sum_{k=1}^{\mathcal{K}} \text{Tr} \left(\bar{\mathbf{U}}_k \mathbf{Y}_k^H \sum_{l=1}^{\mathcal{L}} \hat{\mathbf{H}}_{l,k}^H \mathbf{W}_{l,k} \right) \\
&+ \sum_{k=1}^{\mathcal{K}} \text{Tr} \left(\bar{\mathbf{U}}_k \sum_{l=1}^{\mathcal{L}} \mathbf{W}_{l,k}^H \hat{\mathbf{H}}_{l,k} \mathbf{Y}_k \right) - \sum_{k=1}^{\mathcal{K}} \text{Tr} \left(\bar{\mathbf{U}}_k \mathbf{Y}_k^H \sum_{l=1}^{\mathcal{L}} \sum_{i=1}^{\mathcal{K}} \hat{\mathbf{H}}_{l,k}^H \mathbf{W}_{l,i} \mathbf{W}_{l,i}^H \hat{\mathbf{H}}_{l,k} \mathbf{Y}_k \right) \\
&- \mathbb{E} \left\{ \sum_{k=1}^{\mathcal{K}} \text{Tr} \left(\bar{\mathbf{U}}_k \mathbf{Y}_k^H \sum_{l=1}^{\mathcal{L}} \sum_{i=1}^{\mathcal{K}} \bar{\mathbf{H}}_{l,k}^H \mathbf{W}_{l,i} \mathbf{W}_{l,i}^H \bar{\mathbf{H}}_{l,k} \mathbf{Y}_k \right) \right\} - \sum_{k=1}^{\mathcal{K}} \text{Tr}(\sigma_k^2 \bar{\mathbf{U}}_k \mathbf{Y}_k^H \mathbf{Y}_k).
\end{aligned} \tag{12}$$

where $\bar{\mathbf{U}}_k \triangleq \mathbf{U}_k + \mathbf{I}_{\mathcal{M}_u}, \forall k \in \mathcal{K}$.

Proof. This proposition is extending QT and FPT methods from vector-forms into matrix-forms, and the proof can follow the result in [36], [37], and thus, is omitted here for brevity. \square

Although we have introduced two additional optimization variables, the problem \mathcal{P}_2 has been significantly simplified. However, the problem \mathcal{P}_2 is still hard to solve due to the presence of the expectation operation with respect to the CSI uncertainties $\bar{\mathbf{D}}_{l,k}, \forall l, k$, $\bar{\mathbf{G}}_{r,k}, \forall r, k$, and $\bar{\mathbf{S}}_{l,r}, \forall l, r$. To this end, we first investigate the expectation term and have the following proposition

Proposition 2. *After further employing algebraic manipulations, the expectation term can be expressed by*

$$\begin{aligned}
&\mathbb{E} \left\{ \sum_{k=1}^{\mathcal{K}} \text{Tr} \left(\bar{\mathbf{U}}_k \mathbf{Y}_k^H \sum_{l=1}^{\mathcal{L}} \sum_{i=1}^{\mathcal{K}} \bar{\mathbf{H}}_{l,k}^H \mathbf{W}_{l,i} \mathbf{W}_{l,i}^H \bar{\mathbf{H}}_{l,k} \mathbf{Y}_k \right) \right\} \\
&= \sum_{k=1}^{\mathcal{K}} \sum_{l=1}^{\mathcal{L}} \sum_{i=1}^{\mathcal{K}} \delta_{\mathbf{D}_{l,k}}^2 \text{Tr}(\mathbf{Y}_k \bar{\mathbf{U}}_k \mathbf{Y}_k^H) \text{Tr}(\mathbf{W}_{l,i} \mathbf{W}_{l,i}^H) \\
&\quad + \sum_{k=1}^{\mathcal{K}} \sum_{l=1}^{\mathcal{L}} \sum_{i=1}^{\mathcal{K}} \alpha^2 \delta_{\mathbf{G}_k}^2 \text{Tr}(\mathbf{Y}_k \bar{\mathbf{U}}_k \mathbf{Y}_k^H) \text{Tr}(\hat{\mathbf{S}}_l \mathbf{W}_{l,i} \mathbf{W}_{l,i}^H \hat{\mathbf{S}}_l^H) \\
&\quad + \sum_{k=1}^{\mathcal{K}} \sum_{l=1}^{\mathcal{L}} \sum_{i=1}^{\mathcal{K}} \alpha^2 \delta_{\mathbf{S}_l}^2 \text{Tr}(\hat{\mathbf{G}}_k \mathbf{Y}_k \bar{\mathbf{U}}_k \mathbf{Y}_k^H \hat{\mathbf{G}}_k^H) \text{Tr}(\mathbf{W}_{l,i} \mathbf{W}_{l,i}^H) \\
&\quad + \sum_{k=1}^{\mathcal{K}} \sum_{l=1}^{\mathcal{L}} \sum_{i=1}^{\mathcal{K}} \mathcal{RN} \alpha^2 \delta_{\mathbf{S}_l}^2 \delta_{\mathbf{G}_k}^2 \text{Tr}(\mathbf{Y}_k \bar{\mathbf{U}}_k \mathbf{Y}_k^H) \text{Tr}(\mathbf{W}_{l,i} \mathbf{W}_{l,i}^H).
\end{aligned} \tag{13}$$

From (13), we know the expectation term in (12) with respect to CSI uncertainties is independent of the passive reflecting beamforming. Thus, the expectation term with respect to CSI uncertainties has no direct impact on optimizing of the the passive reflecting beamforming.

Proof. The strict proof is given in Appendix A. \square

Note that the objective function in the problem \mathcal{P}_2 is convex with respect to any one of the four variables $\tilde{\mathbf{U}}, \tilde{\mathbf{Y}}, \tilde{\mathbf{W}}$, and $\tilde{\mathbf{\Theta}}$ when the other three being fixed. Thus, inspired by this fact, in the rest of this section, we decompose the problem \mathcal{P}_2 into several subproblems and solve them

in an alternate manner and then repeatedly until converge. The solutions after the t -th iteration are denoted by $(\cdot)^{(t+1)}$.

A. Optimization of Auxiliary Matrices

First, with fixed variables of $\tilde{\mathbf{W}}^{(t)}$ and $\tilde{\Theta}^{(t)}$, the optimal auxiliary variables $\tilde{\mathbf{Y}}^{(t+1)}$ and $\tilde{\mathbf{U}}^{(t+1)}$ can be determined. Particularly, note that the auxiliary variables $\tilde{\mathbf{Y}}$ and $\tilde{\mathbf{U}}$ only appear in the objective function and do not exist in any constraint sets, which implies that the calculation subproblems of the two auxiliary matrices constitute a pair of unconstrained optimization problems. Thus, the solutions can be obtained by setting the partial derivatives of $f_1(\tilde{\mathbf{W}}, \tilde{\Theta}, \tilde{\mathbf{U}}, \tilde{\mathbf{Y}})$ with respect to $\tilde{\mathbf{Y}}$ and $\tilde{\mathbf{U}}$ to be zeros, respectively.

After the matrix manipulations, the closed-form solution of $\tilde{\mathbf{Y}}$ can be expressed by

$$\mathbf{Y}_k^{(t+1)} = \tilde{\mathbf{V}}_k^{-1} \sum_{l=1}^{\mathcal{L}} \hat{\mathbf{H}}_{l,k}^H \mathbf{W}_{l,k}, \forall k. \quad (14)$$

where

$$\begin{aligned} \tilde{\mathbf{V}}_k = & \sum_{l=1}^{\mathcal{L}} \sum_{i=1}^{\mathcal{K}} \hat{\mathbf{H}}_{l,k}^H \mathbf{W}_{l,i} \mathbf{W}_{l,i}^H \hat{\mathbf{H}}_{l,k} \\ & + \sum_{l=1}^{\mathcal{L}} \sum_{i=1}^{\mathcal{K}} \left(\delta_{\mathbf{D}_{l,k}}^2 \mathbf{I}_{\mathcal{M}_U} + \alpha^2 \delta_{\mathbf{S}_l}^2 \hat{\mathbf{G}}_k^H \hat{\mathbf{G}}_k + \alpha^2 \mathcal{RN} \delta_{\mathbf{G}_k}^2 \delta_{\mathbf{S}_l}^2 \mathbf{I}_{\mathcal{M}_U} \right) \text{Tr}(\mathbf{W}_{l,i} \mathbf{W}_{l,i}^H) \\ & + \sum_{l=1}^{\mathcal{L}} \sum_{i=1}^{\mathcal{K}} \alpha^2 \delta_{\mathbf{G}_k}^2 \mathbf{I}_{\mathcal{M}_U} \text{Tr}(\hat{\mathbf{S}}_l \mathbf{W}_{l,i} \mathbf{W}_{l,i}^H \hat{\mathbf{S}}_l^H) + \sigma_k^2 \mathbf{I}_{\mathcal{M}_U}. \end{aligned} \quad (15)$$

The optimal solution of the auxiliary matrices $\tilde{\mathbf{Y}}$ determined by (14) is known as minimum mean-square error (MMSE) decoding filter [38].

Then, by substituting the obtained optimal solution of $\tilde{\mathbf{Y}}^{(t+1)}$ into $f_1(\tilde{\mathbf{W}}, \tilde{\Theta}, \tilde{\mathbf{U}}, \tilde{\mathbf{Y}})$, the closed-form solution of $\tilde{\mathbf{U}}^{(t+1)}$ can be determined as follows

$$\mathbf{U}_k^{(t+1)} = \sum_{l=1}^{\mathcal{L}} \mathbf{W}_{l,k}^H \hat{\mathbf{H}}_{l,k} \tilde{\mathbf{V}}_k^{-1} \hat{\mathbf{H}}_{l,k}^H \mathbf{W}_{l,k}, \forall k. \quad (16)$$

where $\tilde{\mathbf{V}}_k = \tilde{\mathbf{V}}_k - \sum_{l=1}^{\mathcal{L}} \hat{\mathbf{H}}_{l,k}^H \mathbf{W}_{l,k} \mathbf{W}_{l,k}^H \hat{\mathbf{H}}_{l,k}$.

B. Optimization of Active Transmitting Beamforming

In this subsection, we study the optimization of the active transmitting beamforming $\tilde{\mathbf{W}}$, while fixing $\tilde{\mathbf{Y}}^{(t+1)}$, $\tilde{\mathbf{U}}^{(t+1)}$, and $\tilde{\Theta}^{(t)}$. By omitting the irrelevant constant terms with respect to $\tilde{\mathbf{W}}$, i.e.,

$\sum_{k=1}^{\mathcal{K}} \log |\bar{\mathbf{U}}_k|$, $\sum_{k=1}^{\mathcal{K}} \text{Tr}(\mathbf{U}_k)$, and $\sum_{k=1}^{\mathcal{K}} \text{Tr}(\sigma_k^2 \bar{\mathbf{U}}_k \mathbf{Y}_k^H \mathbf{Y}_k)$, which have no impact on updating of $\tilde{\mathbf{W}}$, the subproblem of optimizing the active transmitting beamforming can be simplified by

$$\begin{aligned} \mathcal{P}_3 : \tilde{\mathbf{W}}^{(t+1)} \triangleq \arg \min_{\tilde{\mathbf{W}}} & \sum_{l=1}^{\mathcal{L}} \sum_{k=1}^{\mathcal{K}} \text{Tr}(\mathbf{W}_{l,k}^H \mathbf{A}_l \mathbf{W}_{l,k}) \\ & - \sum_{l=1}^{\mathcal{L}} \sum_{k=1}^{\mathcal{K}} \text{Tr}(\bar{\mathbf{U}}_k \mathbf{Y}_k^H \hat{\mathbf{H}}_{l,k}^H \mathbf{W}_{l,k}) \\ & - \sum_{l=1}^{\mathcal{L}} \sum_{k=1}^{\mathcal{K}} \text{Tr}(\bar{\mathbf{U}}_k \mathbf{W}_{l,k}^H \hat{\mathbf{H}}_{l,k} \mathbf{Y}_k), \end{aligned} \quad (17a)$$

$$\text{s. t.} \quad \sum_{k=1}^{\mathcal{K}} \text{Tr}(\mathbf{W}_{l,k}^H \mathbf{W}_{l,k}) \leq P_l^{\max}, \forall l \in \mathcal{L}, \quad (17b)$$

where

$$\begin{aligned} \mathbf{A}_l = & \sum_{k=1}^{\mathcal{K}} \hat{\mathbf{H}}_{l,k} \mathbf{Y}_k \bar{\mathbf{U}}_k \mathbf{Y}_k^H \hat{\mathbf{H}}_{l,k}^H + \sum_{k=1}^{\mathcal{K}} \left(\delta_{\mathbf{D}_{l,k}}^2 + \alpha^2 \mathcal{RN} \delta_{\mathbf{G}_k}^2 \delta_{\mathbf{S}_l}^2 \right) \text{Tr}(\mathbf{Y}_k \bar{\mathbf{U}}_k \mathbf{Y}_k^H) \mathbf{I}_{\mathcal{M}_B} \\ & + \sum_{k=1}^{\mathcal{K}} \alpha^2 \delta_{\mathbf{G}_k}^2 \text{Tr}(\mathbf{Y}_k \bar{\mathbf{U}}_k \mathbf{Y}_k^H) \hat{\mathbf{S}}_l^H \hat{\mathbf{S}}_l + \sum_{k=1}^{\mathcal{K}} \alpha^2 \delta_{\mathbf{S}}^2 \text{Tr}(\hat{\mathbf{G}}_k \mathbf{Y}_k \bar{\mathbf{U}}_k \mathbf{Y}_k^H \hat{\mathbf{G}}_k^H) \mathbf{I}_{\mathcal{M}_B}. \end{aligned} \quad (18)$$

It can be verified that the objective function (17a) and the constraint (17b) are both convex with respect to $\tilde{\mathbf{W}}$, thus, the problem \mathcal{P}_3 constitutes a convex optimization problem, which can be efficiently solved by employing the generic convex solvers, e.g., CVX [39]. Instead of relying on the generic solver with high computational complexity, we provide a locally optimal solution in nearly closed-form of $\tilde{\mathbf{W}}$ by employing Lagrangian dual multiplier method [40].

Since the problem \mathcal{P}_3 satisfies the Slater's condition and the dual gap is guaranteed to be zero, thus, the optimal solution can be obtained by solving its dual problem instead of its original one [41]. The Karush–Kuhn–Tucker (KKT) conditions of the problem \mathcal{P}_3 with respect to $\tilde{\mathbf{W}}$ are represented as

$$\nabla_{\mathbf{W}_{l,k}} \mathcal{L}(\tilde{\mathbf{W}}, \tilde{\lambda}) = 2 \frac{\partial \mathcal{L}(\tilde{\mathbf{W}}, \tilde{\lambda})}{\partial \mathbf{W}_{l,k}^*} = \mathbf{0}, \forall l, k, \quad (19a)$$

$$\lambda_l \left(\sum_{k=1}^{\mathcal{K}} \text{Tr}(\mathbf{W}_{l,k}^H(\lambda_l) \mathbf{W}_{l,k}(\lambda_l)) - P_l^{\max} \right) = 0, \forall l, \quad (19b)$$

where $\mathcal{L}(\tilde{\mathbf{W}}, \tilde{\lambda})$ is the Lagrangian dual function of the problem \mathcal{P}_3 and can be expressed by

$$\begin{aligned} \mathcal{L}(\tilde{\mathbf{W}}, \tilde{\lambda}) = & \sum_{l=1}^{\mathcal{L}} \sum_{k=1}^{\mathcal{K}} \text{Tr}(\mathbf{W}_{l,k}^H (\mathbf{A}_l + \lambda_l \mathbf{I}_{\mathcal{M}_B}) \mathbf{W}_{l,k}) - \sum_{l=1}^{\mathcal{L}} \sum_{k=1}^{\mathcal{K}} \text{Tr}(\bar{\mathbf{U}}_k \mathbf{Y}_k^H \hat{\mathbf{H}}_{l,k}^H \mathbf{W}_{l,k}) \\ & - \sum_{l=1}^{\mathcal{L}} \sum_{k=1}^{\mathcal{K}} \text{Tr}(\bar{\mathbf{U}}_k \mathbf{W}_{l,k}^H \hat{\mathbf{H}}_{l,k} \mathbf{Y}_k) - \sum_{l=1}^{\mathcal{L}} \lambda_l P_l^{\max}, \end{aligned} \quad (20)$$

and the Lagrangian multiplier $\lambda_l \geq 0$ is associated with the constraint (17b) for the maximal transmitting power of l -th BS and $\tilde{\lambda} = \{\lambda_l, \forall l\}$ is the collecting of all the dual variables.

Algorithm 1 Bisection Search for Solving Problem \mathcal{P}_3

Input: the bounds λ_l^{ub} and λ_l^{lb} , $\forall l$, threshold ε .

- 1: **If** $g_l(0) \leq 0$ holds, **output** $\mathbf{W}_{l,k}^{(t+1)} \triangleq \mathbf{W}_{l,k}(0)$, $\forall l, k$ and **terminate**;
 - 2: **Calculate** $\lambda_l = (\lambda_l^{\text{ub}} + \lambda_l^{\text{lb}}) / 2$ and $g_l(\lambda_l)$;
 - 3: **If** $g_l(\lambda_l) \leq 0$, set $\lambda_l^{\text{ub}} = \lambda_l$, **otherwise**, set $\lambda_l^{\text{lb}} = \lambda_l$;
 - 4: **If** $|\lambda_l^{\text{ub}} - \lambda_l^{\text{lb}}| \leq \varepsilon$, **output** λ_l and $\mathbf{W}_{l,k}^{(t+1)} \triangleq \mathbf{W}_{l,k}(\lambda_l)$, $\forall l, k$, and then **terminate**.
- Otherwise**, go to step 2.

From the first KKT condition in (19a), the optimal solution of $\mathbf{W}_{l,k}$, $\forall \{l, k\}$ is determined by

$$\mathbf{W}_{l,k}(\lambda_l) = (\mathbf{A}_l + \lambda_l \mathbf{I}_{\mathcal{M}_B})^{-1} \hat{\mathbf{H}}_{l,k} \mathbf{Y}_k \mathbf{U}_k, \forall l, k. \quad (21)$$

The dual variable λ_l should be determined for ensuring the second KKT condition in (19b) are satisfied. Let $g_l(\lambda_l) = \sum_{k=1}^{\mathcal{K}} \text{Tr}(\mathbf{W}_{l,k}^H(\lambda_l) \mathbf{W}_{l,k}(\lambda_l)) - P_l^{\max}$, if the inverse of \mathbf{A}_l exists and $g_l(0) \leq 0$ holds, then the optimal active transmitting beamforming is given as

$$\mathbf{W}_{l,k}^{(t+1)} = \mathbf{W}_{l,k}(0), \forall l, k. \quad (22)$$

Otherwise, we have to find λ_l for ensuring $g_l(\lambda_l) = 0$, i.e.,

$$\sum_{k=1}^{\mathcal{K}} \text{Tr}(\mathbf{W}_{l,k}^H(\lambda_l) \mathbf{W}_{l,k}(\lambda_l)) = P_l^{\max}. \quad (23)$$

Note that $g_l(\lambda_l)$ is a monotonically decreasing function of λ_l , we can find λ_l efficiently by employing the bisection search method [41]. The detailed information for optimizing the active transmitting beamforming matrices are summarized in Algorithm 1.

C. Optimization of Passive Reflecting Beamforming

In this subsection, we consider to optimize $\tilde{\mathbf{\Theta}}$, while fixing the auxiliary matrices $\tilde{\mathbf{U}}^{(t+1)}$ and $\tilde{\mathbf{Y}}^{(t+1)}$, and the active transmitting beamforming $\tilde{\mathbf{W}}^{(t+1)}$. First, for the convenience of representation, we define the following matrix merging operations:

$$\mathbf{W}_i = [\mathbf{W}_{1,i}^T, \mathbf{W}_{2,i}^T, \dots, \mathbf{W}_{\mathcal{L},i}^T]^T \in \mathbb{C}^{\mathcal{L}\mathcal{M}_B \times \mathcal{M}_U}, \quad (24a)$$

$$\hat{\mathbf{D}}_k = [\hat{\mathbf{D}}_{1,k}^T, \hat{\mathbf{D}}_{2,k}^T, \dots, \hat{\mathbf{D}}_{\mathcal{L},k}^T]^T \in \mathbb{C}^{\mathcal{L}\mathcal{M}_B \times \mathcal{M}_U}, \quad (24b)$$

$$\hat{\mathbf{S}} = [\hat{\mathbf{S}}_1, \hat{\mathbf{S}}_2, \dots, \hat{\mathbf{S}}_{\mathcal{L}}] \in \mathbb{C}^{\tilde{\mathcal{N}} \times \mathcal{L}\mathcal{M}_B}, \quad (24c)$$

where $\tilde{\mathcal{N}} \triangleq \mathcal{RN}$. Then, by defining $\mathbf{W} = \sum_{i=1}^{\mathcal{K}} \mathbf{W}_i \mathbf{W}_i^H$, we have

$$\sum_{l=1}^{\mathcal{L}} \hat{\mathbf{H}}_{l,k}^H \mathbf{W}_{l,k} = \hat{\mathbf{D}}_k^H \mathbf{W}_k + \hat{\mathbf{G}}_k^H \Theta \hat{\mathbf{S}} \mathbf{W}_k, \quad (25a)$$

$$\begin{aligned} \sum_{l=1}^{\mathcal{L}} \sum_{i=1}^{\mathcal{K}} \hat{\mathbf{H}}_{l,k}^H \mathbf{W}_{l,i} \mathbf{W}_{l,i}^H \hat{\mathbf{H}}_{l,k} &= \hat{\mathbf{D}}_k^H \mathbf{W} \hat{\mathbf{D}}_k + \hat{\mathbf{D}}_k^H \mathbf{W} \hat{\mathbf{S}}^H \Theta^H \hat{\mathbf{G}}_k \\ &+ \hat{\mathbf{G}}_k^H \Theta \hat{\mathbf{S}} \mathbf{W} \hat{\mathbf{D}}_k + \hat{\mathbf{G}}_k^H \Theta \hat{\mathbf{S}} \mathbf{W} \hat{\mathbf{S}}^H \Theta^H \hat{\mathbf{G}}_k. \end{aligned} \quad (25b)$$

By substituting (25) into $f_1(\tilde{\mathbf{W}}, \tilde{\Theta}, \tilde{\mathbf{U}}, \tilde{\mathbf{Y}})$ and omitting irrelevant constants with respect to $\tilde{\Theta}$, i.e., $\sum_{k=1}^{\mathcal{K}} \text{Tr}(\bar{\mathbf{U}}_k \mathbf{Y}_k^H \mathbf{D}_k^H \mathbf{W} \mathbf{D}_k \mathbf{Y}_k)$, $\sum_{k=1}^{\mathcal{K}} \text{Tr}(\bar{\mathbf{U}}_k \mathbf{Y}_k^H \mathbf{D}_k^H \mathbf{W}_k)$, $\sum_{k=1}^{\mathcal{K}} \text{Tr}(\bar{\mathbf{U}}_k \mathbf{W}_k^H \mathbf{D}_k \mathbf{Y}_k)$, and $\sum_{k=1}^{\mathcal{K}} \text{Tr}(\sigma_k^2 \bar{\mathbf{U}}_k \mathbf{Y}_k^H \mathbf{Y}_k)$, which have no impact on optimizing the passive reflecting beamforming at IRSs, we have the following simplified problem with respect to $\tilde{\Theta}$:

$$\begin{aligned} \mathcal{P}_4 : \tilde{\Theta}^{(t+1)} &\triangleq \arg \min_{\tilde{\Theta}} \sum_{k=1}^{\mathcal{K}} \text{Tr}(\bar{\mathbf{U}}_k \mathbf{Y}_k^H \hat{\mathbf{G}}_k^H \Theta \hat{\mathbf{S}} \mathbf{W}_k) \\ &+ \sum_{k=1}^{\mathcal{K}} \text{Tr}(\bar{\mathbf{U}}_k \mathbf{W}_k^H \hat{\mathbf{S}}^H \Theta^H \hat{\mathbf{G}}_k \mathbf{Y}_k) \\ &- \sum_{k=1}^{\mathcal{K}} \text{Tr}(\bar{\mathbf{U}}_k \mathbf{Y}_k^H \hat{\mathbf{G}}_k^H \Theta \hat{\mathbf{S}} \mathbf{W} \hat{\mathbf{S}}^H \Theta^H \hat{\mathbf{G}}_k \mathbf{Y}_k) \\ &- \sum_{k=1}^{\mathcal{K}} \text{Tr}(\bar{\mathbf{U}}_k \mathbf{Y}_k^H \hat{\mathbf{G}}_k^H \Theta \hat{\mathbf{S}} \mathbf{W} \hat{\mathbf{D}}_k \mathbf{Y}_k) \\ &- \sum_{k=1}^{\mathcal{K}} \text{Tr}(\bar{\mathbf{U}}_k \mathbf{Y}_k^H \hat{\mathbf{D}}_k^H \mathbf{W} \hat{\mathbf{S}}^H \Theta^H \hat{\mathbf{G}}_k \mathbf{Y}_k), \end{aligned} \quad (26a)$$

$$\text{s. t. } |\Theta_{n,n}| = \alpha, \forall n \in \tilde{\mathcal{N}}. \quad (26b)$$

The above problem is still arduous to tackle. As follows, we transform the problem \mathcal{P}_4 into an equivalent but more tractable form by employing some further algebraic manipulations.

First, by defining $\mathbf{Z}_k = \hat{\mathbf{G}}_k \mathbf{Y}_k \bar{\mathbf{U}}_k \mathbf{Y}_k^H \hat{\mathbf{G}}_k^H$, $\mathbf{Z} = \sum_{k=1}^{\mathcal{K}} \mathbf{Z}_k$, and $\mathbf{Q} = \hat{\mathbf{S}} \mathbf{W} \hat{\mathbf{S}}^H$, we have

$$\sum_{k=1}^{\mathcal{K}} \text{Tr}(\bar{\mathbf{U}}_k \mathbf{Y}_k^H \hat{\mathbf{G}}_k^H \Theta \hat{\mathbf{S}} \mathbf{W} \hat{\mathbf{S}}^H \Theta^H \hat{\mathbf{G}}_k \mathbf{Y}_k) = \text{Tr}(\Theta^H \mathbf{Z} \Theta \mathbf{Q}). \quad (27)$$

Then, by defining $\mathbf{C}_k = \hat{\mathbf{G}}_k \mathbf{Y}_k \bar{\mathbf{U}}_k \mathbf{Y}_k^H \hat{\mathbf{D}}_k^H \mathbf{W} \hat{\mathbf{S}}^H$ and $\mathbf{C} = \sum_{k=1}^{\mathcal{K}} \mathbf{C}_k$, we have

$$\sum_{k=1}^{\mathcal{K}} \text{Tr}(\bar{\mathbf{U}}_k \mathbf{Y}_k^H \hat{\mathbf{D}}_k^H \mathbf{W} \hat{\mathbf{S}}^H \Theta^H \hat{\mathbf{G}}_k \mathbf{Y}_k) = \text{Tr}(\Theta^H \mathbf{C}), \quad (28a)$$

$$\sum_{k=1}^{\mathcal{K}} \text{Tr}(\bar{\mathbf{U}}_k \mathbf{Y}_k^H \hat{\mathbf{G}}_k^H \Theta \hat{\mathbf{S}} \mathbf{W} \hat{\mathbf{D}}_k \mathbf{Y}_k) = \text{Tr}(\mathbf{C}^H \Theta). \quad (28b)$$

Next, by defining $\mathbf{E}_k = \hat{\mathbf{G}}_k \mathbf{Y}_k \bar{\mathbf{U}}_k \mathbf{W}_k^H \hat{\mathbf{S}}^H$ and $\mathbf{E} = \sum_{k=1}^{\mathcal{K}} \mathbf{E}_k$, we have

$$\sum_{k=1}^{\mathcal{K}} \text{Tr}(\bar{\mathbf{U}}_k \mathbf{W}_k^H \hat{\mathbf{S}}^H \Theta^H \hat{\mathbf{G}}_k \mathbf{Y}_k) = \text{Tr}(\Theta^H \mathbf{E}), \quad (29a)$$

$$\sum_{k=1}^{\mathcal{K}} \text{Tr}(\bar{\mathbf{U}}_k \mathbf{Y}_k^H \hat{\mathbf{G}}_k^H \Theta \hat{\mathbf{S}} \mathbf{W}_k) = \text{Tr}(\mathbf{E}^H \Theta). \quad (29b)$$

Equivalently, we have a sequence of equalities as follows

$$\text{Tr}(\Theta^H \mathbf{Z} \Theta \mathbf{Q}) = \boldsymbol{\theta}^H \mathbf{Z} \boldsymbol{\theta}, \quad \text{Tr}(\Theta^H \Omega) = \boldsymbol{\theta}^H \boldsymbol{\omega}, \quad (30)$$

where $\mathbf{Z} \triangleq \mathbf{Z} \odot \mathbf{Q}^T \in \mathbb{C}^{\tilde{\mathcal{N}} \times \tilde{\mathcal{N}}}$, $\Omega = \mathbf{E} - \mathbf{C} \in \mathbb{C}^{\tilde{\mathcal{N}} \times \tilde{\mathcal{N}}}$,

$$\boldsymbol{\theta} = \text{Vecd}(\Theta) \in \mathbb{C}^{\tilde{\mathcal{N}} \times 1}, \quad \boldsymbol{\omega} = \text{Vecd}(\Omega) \in \mathbb{C}^{\tilde{\mathcal{N}} \times 1}, \quad (31)$$

where $\text{Vecd}(\mathbf{X})$ forms a vector out of the diagonal of its matrix argument. The sequence of equalities given above in (30) follow from the properties in [42, Theorem 1.11].

Then, based on the aforementioned equivalent transformations, the problem \mathcal{P}_4 can be reformulated by

$$\mathcal{P}_5 : \tilde{\boldsymbol{\theta}}^{(t+1)} \triangleq \max_{\tilde{\boldsymbol{\theta}}} \quad -\boldsymbol{\theta}^H \mathbf{Z} \boldsymbol{\theta} + \boldsymbol{\theta}^H \boldsymbol{\omega} + \boldsymbol{\omega}^H \boldsymbol{\theta} \quad (32a)$$

$$\text{s. t.} \quad |\boldsymbol{\theta}_n| = \alpha, n = 1, 2, \dots, \tilde{\mathcal{N}}. \quad (32b)$$

Due to the non-convexity of the constant modulus constraints in (32b), the above optimization problem is still non-convex, and belongs to the class of NP-hard problems. The widely employed methods to solve the problem \mathcal{P}_5 with high-quality suboptimal solution are employing semidefinite relaxation [12] or quadratic relaxation [8], however, both the relaxation-based techniques suffer from high computational complexities, i.e., the order are larger than $\mathcal{O}(\mathcal{R}^6 \mathcal{N}^6)$. In practice, since $\mathcal{R} \times \mathcal{N}$ is large, it is computational impractical in real world. Hence, in the following, we provide a low complexity alternate sequential optimization (ASO) algorithm [43] to solve this non-convex problem.

Note that the objective function (32a) and the constant modulus constraints (32b) in the problem \mathcal{P}_5 are separable with respect to $\boldsymbol{\theta}_i, \forall i \in \tilde{\mathcal{N}}$ [11], [12], therefore, we can decompose the problem \mathcal{P}_5 into $\tilde{\mathcal{N}}$ separate subproblems and solve them one-by-one. Particularly, we have

$$\boldsymbol{\theta}^H \boldsymbol{\omega} = \sum_{n=1}^{\tilde{\mathcal{N}}} \boldsymbol{\theta}_n^* \omega_n = \boldsymbol{\theta}_i^* \omega_i + \sum_{\substack{n=1 \\ n \neq i}}^{\tilde{\mathcal{N}}} \boldsymbol{\theta}_n^* \omega_n. \quad (33)$$

Meanwhile, $\boldsymbol{\theta}^H \mathbf{Z} \boldsymbol{\theta}$ can be expanded as

$$\begin{aligned} \boldsymbol{\theta}^H \mathbf{Z} \boldsymbol{\theta} &= \sum_{\substack{n=1 \\ n \neq i}}^{\tilde{\mathcal{N}}} \boldsymbol{\theta}^H \mathbf{z}_n \boldsymbol{\theta}_n + \boldsymbol{\theta}^H \mathbf{z}_i \boldsymbol{\theta}_i \\ &= \sum_{\substack{n=1 \\ n \neq i}}^{\tilde{\mathcal{N}}} \boldsymbol{\theta}_i^* z_{i,n} \boldsymbol{\theta}_n + \boldsymbol{\theta}^H \mathbf{z}_i \boldsymbol{\theta}_i + \sum_{\substack{m=1 \\ m \neq n}}^{\tilde{\mathcal{N}}} \sum_{\substack{p=1 \\ p \neq i}}^{\tilde{\mathcal{N}}} \boldsymbol{\theta}_m^* z_{m,p} \boldsymbol{\theta}_p \\ &= \boldsymbol{\theta}_i^* z_{i,i} \boldsymbol{\theta}_i + \sum_{\substack{n=1 \\ n \neq i}}^{\tilde{\mathcal{N}}} (\boldsymbol{\theta}_i^* z_{i,n} \boldsymbol{\theta}_n + \boldsymbol{\theta}_i z_{n,i} \boldsymbol{\theta}_n^*) + \sum_{\substack{m=1 \\ m \neq n}}^{\tilde{\mathcal{N}}} \sum_{\substack{p=1 \\ p \neq i}}^{\tilde{\mathcal{N}}} \boldsymbol{\theta}_m^* z_{m,p} \boldsymbol{\theta}_p, \end{aligned} \quad (34)$$

where $\mathbf{Z} = [\mathbf{z}_1, \mathbf{z}_2, \dots, \mathbf{z}_{\tilde{N}}]$ with $\mathbf{z}_n = [z_{1,n}, z_{2,n}, \dots, z_{\tilde{N},n}]^T \in \mathbb{C}^{\tilde{N} \times 1}$. By using the property $z_{i,n} = z_{n,i}^*$ and basing on the fact that \mathbf{Z} is a positive semi-definite matrix, we have

$$\begin{aligned} & -\boldsymbol{\theta}^H \mathbf{Z} \boldsymbol{\theta} + \boldsymbol{\theta}^H \boldsymbol{\omega} + \boldsymbol{\omega}^H \boldsymbol{\theta} \\ &= 2 \operatorname{Re} \left\{ \boldsymbol{\theta}_i^* \boldsymbol{\omega}_i + \sum_{\substack{n=1 \\ n \neq i}}^{\tilde{N}} \boldsymbol{\theta}_n^* \boldsymbol{\omega}_n - \sum_{\substack{n=1 \\ n \neq i}}^{\tilde{N}} \boldsymbol{\theta}_i^* z_{i,n} \boldsymbol{\theta}_n \right\} - \boldsymbol{\theta}_i^* z_{i,i} \boldsymbol{\theta}_i - \sum_{\substack{m=1 \\ m \neq n}}^{\tilde{N}} \sum_{\substack{p=1 \\ p \neq i}}^{\tilde{N}} \boldsymbol{\theta}_m^* z_{m,p} \boldsymbol{\theta}_p \\ &\triangleq 2 \operatorname{Re} \{ \boldsymbol{\theta}_i^* \boldsymbol{\mu}_i \} + \boldsymbol{\xi} \end{aligned} \quad (35)$$

where

$$\boldsymbol{\mu}_i = \boldsymbol{\omega}_i - \sum_{\substack{n=1 \\ n \neq i}}^{\tilde{N}} z_{i,n} \boldsymbol{\theta}_n, \quad (36a)$$

$$\boldsymbol{\xi} = 2 \operatorname{Re} \left\{ \sum_{\substack{n=1 \\ n \neq i}}^{\tilde{N}} \boldsymbol{\theta}_n^* \boldsymbol{\omega}_n \right\} - \sum_{\substack{m=1 \\ m \neq n}}^{\tilde{N}} \sum_{\substack{p=1 \\ p \neq i}}^{\tilde{N}} \boldsymbol{\theta}_m^* z_{m,p} \boldsymbol{\theta}_p - \boldsymbol{\theta}_i^* z_{i,i} \boldsymbol{\theta}_i, \quad (36b)$$

where $\boldsymbol{\xi}$ is the irreverent constant term with regard to $\boldsymbol{\theta}_i$ (e.g., $\boldsymbol{\theta}_i^* z_{i,i} \boldsymbol{\theta}_i = z_{i,i} |\boldsymbol{\theta}_i|^2 = \alpha^2 z_{i,i}$), which do not affect the optimal solution. Thus, we can only investigate $\operatorname{Re} \{ \boldsymbol{\theta}_i^* \boldsymbol{\mu}_i \}$ for sequentially optimizing each PS while fixing the remaining $\tilde{N} - 1$ PSs. Hence, we have

$$\mathcal{P}_6 : \max_{\boldsymbol{\theta}_i} \operatorname{Re} \{ \boldsymbol{\theta}_i^* \boldsymbol{\mu}_i \} \quad (37a)$$

$$\text{s. t. } |\boldsymbol{\theta}_i| = \alpha, \quad (37b)$$

An equivalent expression for the above problem is given by

$$\mathcal{P}_7 : \max_{\phi_i} \cos(-\phi_i + \eta_i) \quad (38a)$$

$$\text{s. t. } \phi_i \in [0, 2\pi], \quad (38b)$$

where η_i and $-\phi_i$ are the phase-shifting of $\boldsymbol{\mu}_i$ and $\boldsymbol{\theta}_i^*$, respectively. Thus, the problem \mathcal{P}_7 has a closed-form optimal, which is given by

$$\phi_i = \eta_i, \forall i \in \tilde{N}. \quad (39)$$

Accordingly, we have

$$\boldsymbol{\theta}_i = \alpha e^{j\eta_i}, \forall i \in \tilde{N}. \quad (40)$$

Based on the above discussions, the procedure of sequentially optimizing $\boldsymbol{\theta}_1, \boldsymbol{\theta}_2, \dots, \boldsymbol{\theta}_{\tilde{N}}$ and then repeatedly until the convergence is attained. The details for optimizing the locally optimal passive reflecting beamforming by employing ASO algorithm are summarized in Algorithm 2, and we have the following lemma

Algorithm 2 ASO Algorithm for Optimizing the Passive Reflecting Beamforming

Input: \mathcal{Z} , threshold ε , $\theta^0 \triangleq \theta^{(t)}$, $u = 1$.

- 1: **Sequentially Calculate** $\theta_i^u, \forall i \in \tilde{\mathcal{N}}$, by using (40);
 - 2: **Calculate** $\rho^u = -(\theta^u)^H \mathcal{Z} \theta + (\theta^u)^H \omega + \omega^H \theta^u$;
 - 3: **If** $|\rho^{u+1} - \rho^u| \leq \varepsilon$, **output** $\theta^{(t+1)} \triangleq \theta^u$ and then **terminate**;
 - Otherwise**, update $u \leftarrow u + 1$ and go to Step 1.
-

Algorithm 3 RJD Algorithm for Solving Problem \mathcal{P}_1

Input: $\tilde{\mathbf{W}}^{(0)}$, $\tilde{\Theta}^{(0)}$; threshold ε , $t = 0$.

- 1: **Calculate** $\tilde{\mathbf{Y}}^{(t+1)}$ by using (14);
 - 2: **Calculate** $\tilde{\mathbf{U}}^{(t+1)}$, by using (16);
 - 3: **Calculate** $\tilde{\mathbf{W}}^{(t+1)}$, by employing Algorithm 1;
 - 4: **Calculate** $\tilde{\Theta}^{(t+1)}$, by employing Algorithm 2;
 - If** $|\mathcal{R}^{(t+1)} - \mathcal{R}^{(t)}| < \varepsilon$, **output** $\tilde{\mathbf{W}}_{l,k}^{\text{opt}} \triangleq \tilde{\mathbf{W}}^{(t)}$ and $\tilde{\Theta}^{\text{opt}} \triangleq \tilde{\Theta}^{(t)}$, and then **terminate**;
 - Otherwise**, update $t \leftarrow t + 1$, and go to step 1.
-

Lemma 1. *Algorithm 2 is guaranteed to converge.*

Proof. The proof is presented in Appendix B □

D. Analysis of the Overall Algorithm

The details of the proposed robust joint design (RJD) algorithm are summarized in Algorithm 3. The convergence of the proposed RJD algorithm can be guaranteed since the average sum-rate $\mathcal{R}(\tilde{\mathbf{W}}, \tilde{\Theta})$ is monotonically non-decreasing after each updating step in Algorithm 3. Overall, it can be summarized that

$$\mathcal{R}(\tilde{\mathbf{W}}^{(t+1)}, \tilde{\Theta}^{(t+1)}) \geq \mathcal{R}(\tilde{\mathbf{W}}^{(t+1)}, \tilde{\Theta}^{(t)}) \geq \mathcal{R}(\tilde{\mathbf{W}}^{(t)}, \tilde{\Theta}^{(t)}) \geq \dots \geq \mathcal{R}(\tilde{\mathbf{W}}^{(1)}, \tilde{\Theta}^{(1)}). \quad (41)$$

Besides, $\mathcal{R}(\tilde{\mathbf{W}}, \tilde{\Theta})$ is upper-bounded by a finite value due to the limited transmit powers of BSs and the finite number of PSs of IRSs. As the number of iterations increases, we finally have $\mathcal{R}(\tilde{\mathbf{W}}^{\text{opt}}, \tilde{\Theta}^{\text{opt}}) \triangleq \mathcal{R}(\tilde{\mathbf{W}}^{(t_{\max})}, \tilde{\Theta}^{(t_{\max})})$, where t_{\max} is the maximal number of iterations when Algorithm 3 converges.

Meanwhile, the complexity of Algorithm 3 is briefly discuss as follows. The complexities of updating \mathbf{U}_k and \mathbf{Y}_k are on the order of $\mathcal{O}(\mathcal{M}_U^3), \forall k$, respectively. The complexity of calculating $\mathbf{W}_{l,k}$ is $\mathcal{O}(\mathcal{M}_B^3), \forall l, k$, and the complexity of updating Θ is $\mathcal{O}(\mathcal{R}^2\mathcal{N}^2)$. Therefore, based on the aforementioned discussions, the total complexity of Algorithm 3 is $\mathcal{O}(\mathcal{I}_3(2\mathcal{K}\mathcal{M}_U^3 + \mathcal{I}_1\mathcal{L}\mathcal{K}\mathcal{M}_B^3 + \mathcal{I}_2\mathcal{R}^2\mathcal{N}^2))$, where $\mathcal{I}_1, \mathcal{I}_2$ and \mathcal{I}_3 are the number of iterations when Algorithm 1, Algorithm 2 and Algorithm 3 converge, respectively.

IV. NUMERICAL SIMULATION AND DISCUSSION

As follows, simulation results are provided to evaluate the performance of the proposed RJD algorithm. We consider a system schematic as shown in Fig. 2, a three-IRSs assisted cell-free wireless communication network, where six-BSs are transmitting signals to four-UEs cooperatively. We assume a 3-D scenario, where the height of the BSs, the IRSs, and the UEs are 3m, 6m, and 1.5m, respectively. The four UEs are uniformly and randomly distributed in a circle centered at $(\chi, 100)$ with a radius of 10m and the locations of BSs and IRSs are shown in Fig. 2. The distance-dependent large-scale path loss is denoted by

$$L(d_x) = \mathcal{C}_0 (d_x/d_0)^{-p_x}, \quad (42)$$

where $\mathcal{C}_0 = -30$ dB is the channel power gain at the reference distance $d_0 = 1$ m, and d_x and p_x denote the link distance and path loss exponent. We set $p_{D_{l,k}} = 3.75, \forall l, k$, $p_{S_{l,r}} = p_{G_{r,k}} = 2.2, \forall l, k, r$. Meanwhile, we assume the PSs along the horizontal and vertical are $\mathcal{N}_h = 10$ and $\mathcal{N}_v = \mathcal{N}/\mathcal{N}_h$, respectively. The noise variance at each UE is $\sigma_k^2 = \sigma^2 = -90$ dBm. For the statistical CSI error model, the normalized CSI errors are set as $\kappa^2 = \kappa_D^2 = \kappa_S^2 = \kappa_F^2 = 0.001$. Unless otherwise stated, the other simulation parameters used in the rest of this section are setting as $\mathcal{M}_B = 4$, $\mathcal{M}_U = 2$, $\mathcal{N} = 20$, $\alpha = 1$, $P_l^{\max} = 0.1$ W, and the Rician factors are $\beta_G = \beta_S = 3$.

Furthermore, in practice, the phase-shifting of each PS can only take finite discrete value from the discrete phase-shifting set [12], [14]. Let b denote the number of bits to represent the resolution levels of IRS, the discrete phase-shifting set is represented by

$$\phi_{\mathcal{D}} \in \mathcal{D} \triangleq \left\{ \frac{2\pi g}{2^b} \mid g = 0, 1, 2, \dots, 2^b - 1 \right\}. \quad (43)$$

To our best knowledge, the only way to obtain the global optimal from the discrete set is to perform exhaustive search, and the computational complex is $\mathcal{O}(2^{b\mathcal{RN}})$, i.e., exponential

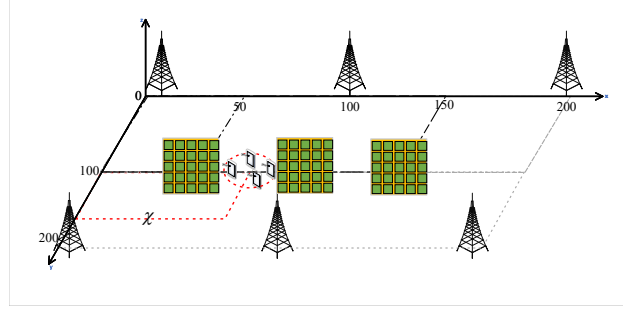


Fig. 2. IRSs-assisted cell-free MIMO communication network scenario.

increasing with respect to the number of PSs of IRSs $\mathcal{R} \times \mathcal{N}$ and the IRS resolution b bits. In practice, since $\mathcal{R} \times \mathcal{N}$ is large, it is computational impractical in real world. As a compromising approach, the common way to obtain the local optimal discrete phase-shifting of PS is projecting the continuous phase-shifting ϕ_n^C obtained by (40) to the nearest discrete value in the set \mathcal{D} , which has been widely employed in existing works [44]. It is computational efficient, i.e., $\mathcal{O}(\mathcal{R}^2 \mathcal{N}^2 \times 2^b)$, and is much smaller than $\mathcal{O}(2^{b\mathcal{R}\mathcal{N}})$.

In the following simulations, we investigate the proposed RJD algorithm under the continuous phase-shifting case and the discrete phase-shifting case of 2-bits and 1-bit, i.e., *RJD, Continuous*, *RJD, 2-bits*, and *RJD, 1-bit*. Meanwhile, all the simulation results are obtained by averaging 500 channel realizations. In the rest section, we investigate the convergence behavior and the impacts of the critical simulation parameters on the performance gains achieved by the proposed RJD algorithms as mentioned above, including *RJD, Continuous*, *RJD, 2-bits*, and *RJD, 1-bit*.

A. Convergence Behavior

In this subsection, we investigate the convergence behavior of the proposed RJD algorithms. As shown in Fig. 3, we plot the curves of the average sum-rate achieved by the proposed RJD schemes against the number of iterations under the different number of PSs at each IRS, i.e., $\mathcal{N} = 20$ and $\mathcal{N} = 50$. The curves are consistent with our expectation, where the three schemes converge to stationary points after a few iterations. It is observed that the convergence speed is sensitive to the number of PSs at each IRS, where the proposed RJD schemes under $\mathcal{N} = 50$ is slower than that under $\mathcal{N} = 20$. Besides, since the size of the discrete phase-shifting set 2^b is much small than $\mathcal{R}^2 \mathcal{N}^2$, thus it has a limited impact on the convergence speed, and the curves of *RJD, 2-bits* and *RJD, 1-bit* schemes also proof this analysis.

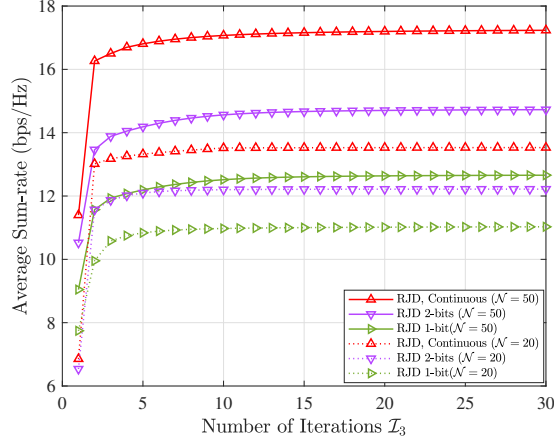


Fig. 3. Average sum-rate against the number of iterations.

B. Performance Comparison and Discussions

To evaluate the performance gain achieved by the IRS, we introduce the conventional cell-free scheme without the aid of IRSs [26], which can be solved by employing Algorithm 3 after setting the reflecting efficiency of all IRSs as zeros, i.e., $\alpha = 0$, and is denoted by *Conventional CF*. Additional, *Upper Bound* scheme is also considered to denote the perfect CSI case.

1) *Impact of the CSI estimation error* : First, we study the impact of the normalized CSI error covariances on the average sum-rate. As shown in Fig. 4(a), we set the normalized CSI errors of all channels are equal, i.e., $\kappa_D^2 = \kappa_S^2 = \kappa_F^2 = \kappa^2$, and investigate the average sum-rate achieved by all schemes against the normalized CSI error. It can be observed that with increasing κ^2 , the performance gaps between all schemes with *Upper Bound* become larger, which is consistent with the expectation. Besides, the performance loss of the proposed RJD schemes (include *RJD*, *Continuous*, *RJD*, *2-bits*, and *RJD*, *1-bit*) are larger than *Conventional CF* with respect to κ^2 , which is due to the channel dimensions in the conventional cell-free network is much smaller than that in the IRS-assisted cell-free network under the considered system setting.

Then, we study the impact of each type of the channel with the different normalized CSI error level on the average sum-rate. As shown in Fig. 4(b), we plot the average sum-rate achieved by the proposed *RJD*, *Continuous* scheme with the different number of PSs. It can be observed that the performance loss is sensitive to the number of PSs of each IRS. Most importantly, the normalized CSI error of the channel from the BS to the IRS, i.e., $S_{l,r}, \forall l, r$ has the largest impact on the average sum-rate due to that the number of antennas at each BS and the number of PSs

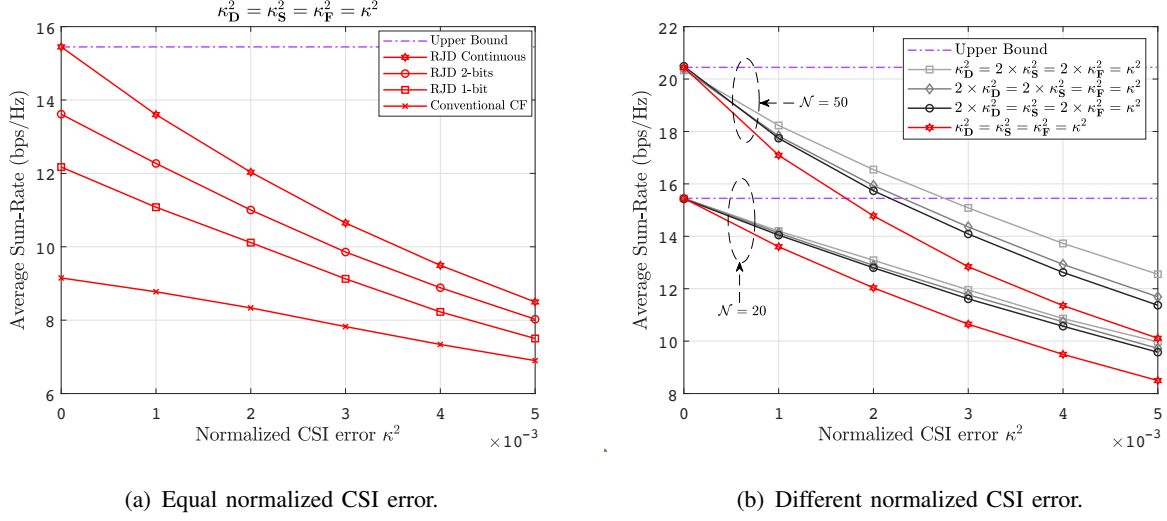


Fig. 4. Average sum-rate against the normalized CSI error.

at each IRS are large, so the aggregate CSI uncertainty increase alongside the corresponding channel dimension. Thus, as the normalized CSI error becomes larger, the performance gap gradually expands. Fortunately, due to the positions of the BSs and the IRSs are fixed, so the CSI knowledge between the BSs and the IRSs can be estimated with satisfactory accuracy by employing the angles of arrival and departure [21].

2) *Impact of the number of PSs at each IRS:* We present the average sum-rates achieved by all schemes against the number of the PSs at each IRS under a pair of normalized CSI errors in Fig. 5. It illustrates that IRSs can considerably improve the performance compared with the conventional cell-free system, i.e., *Conventional CF*, whereby the increasing number of PSs, the performance achieved by the IRS-related schemes (including *Upper Bound*, *RJD*, *Continuous*, *RJD*, *2-bits*, and *RJD*, *1-bit*) increase. The trend of the curves highlights the importance of utilizing IRSs. Besides, the size of the discrete phase-shifting set impacts the performance, and as expected, with increasing \mathcal{N} , the performance gaps between *RJD*, *2-bits* and *RJD*, *1-bit* become larger. The performance loss compared with *RJD*, *Continuous* can be compensated by adopting high-resolution discrete PSs. Most importantly, while the overall trends of the curves resemble those of expectation, an interesting observation can be made. Particularly, when \mathcal{N} increased, although the performance gaps between the proposed *RJD* schemes and *Upper Bound* become large, the slopes of the proposed *RJD* schemes curves towards decrease, which can be attributed to that with the imperfect CSI knowledge, a large number of PSs also means a large

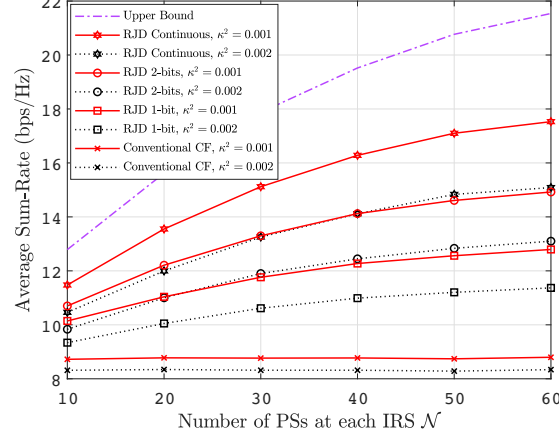


Fig. 5. Average sum-rate against the number of PSs at each IRS.

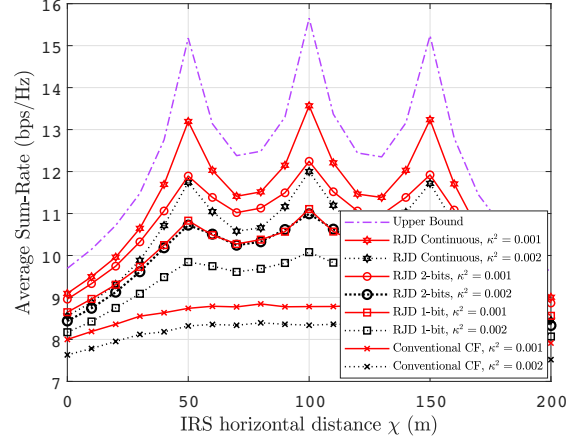


Fig. 6. Average sum-rate against the location of the IRS.

CSI uncertainty, thus the relative performance gain also decreased.

3) *Impact of the UEs location:* We investigate the impact of the UEs location in Fig. 6 while the locations of BSs and UEs remain fixed. The curves are approximately symmetric with respect to the line of $\chi = 100\text{m}$, which are consistent with the expectation. It is observed that as the UEs are deployed closer to each IRS, i.e., $\chi = 50\text{m}$, $\chi = 100\text{m}$, and $\chi = 150\text{m}$, the IRS-related schemes achieve the best performances, which is due to the smaller reflection channel fading. This indicates that the system performance can indeed be improved significantly with the deployment of IRSs, especially when the UEs are closed to the IRS.

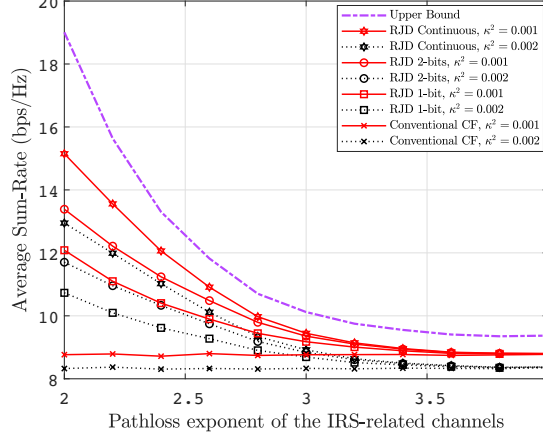


Fig. 7. Average sum-rate against the pathloss exponent of the IRS-related channels.

4) *Impact of the path loss exponent:* We investigate the impact of the path loss exponent of the IRS-related channels while fixing that of direct channels. As shown in Fig. 7, the average sum-rate achieved by all IRS-related schemes decrease significantly with the increasing of the path loss exponent, and finally (i.e., $\rho \geq 3.6$), the curves are approximately coinciding with *Conventional CF*. This is mainly due to that when the path loss exponents of IRS-related channels are large, the array gains introduced by IRS are negligible. To this end, the location of the IRS should be appropriately chosen for ensuring a free space IRS-related channels can be established, which thus to establish reliable communication links between BSs and UEs.

5) *Impact of the reflecting efficiency:* Fig. 8 illustrates the average sum-rate against the reflecting efficiency of IRSs. The comparative performance patterns are similar to Fig. 5. It can be observed that the reflecting efficiency of IRS has a substantial impact on the performance, where as expected, with the increasing α , the average sum-rate achieved by IRS-related schemes increased significantly. It can be attributed to that a larger α means the fewer power loss caused by signal absorption at IRSs.

V. CONCLUSION

In this paper, we proposed robust joint design the IRS-assisted cell-free network. Particularly, we adopted a stochastic method to cope with the CSI uncertainty by maximizing the expectation of the sum-rate, which guaranteed the robust performance over the average. Accordingly, we formulated an average sum-rate maximization problem and further transformed it into an equiv-

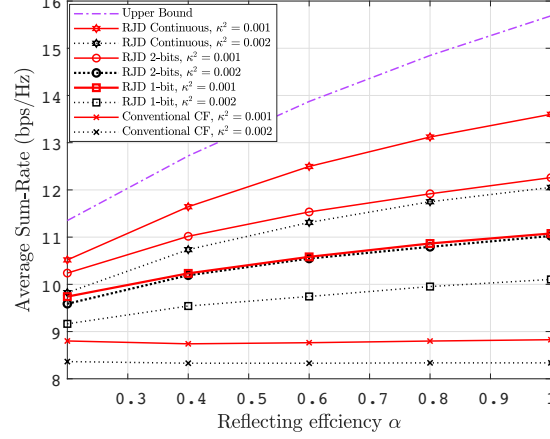


Fig. 8. Average sum-rate against the reflecting efficiency.

alent but more tractable form after employing algebraic manipulations. Then, the transformed problem was decomposed into two subproblems with respect to active and passive beamforming matrices of BSs and IRSs. We also proved that the expectation value with respect to CSI uncertainties has no direct impact on optimizing of passive reflecting beamforming matrices of IRSs. Further, the two subproblems could be solved alternating iteratively and obtained the locally optimal solutions in nearly closed-forms. Simulation results confirmed that deploying IRSs can considerably enhance the data rate compared with conventional cell-free networks and the proposed robust joint design algorithm has the robustness against the CSI uncertainty.

APPENDIX

A. Proof of Proposition 2

By substituting (4) into the expectation term, we have

$$\begin{aligned}
& \mathbb{E} \left\{ \sum_{k=1}^{\mathcal{K}} \text{Tr} \left(\bar{\mathbf{U}}_k \mathbf{Y}_k^H \sum_{l=1}^{\mathcal{L}} \sum_{i=1}^{\mathcal{K}} \bar{\mathbf{H}}_{l,k}^H \mathbf{W}_{l,i} \mathbf{W}_{l,i}^H \bar{\mathbf{H}}_{l,k} \mathbf{Y}_k \right) \right\} \\
&= \underbrace{\mathbb{E} \left\{ \sum_{k=1}^{\mathcal{K}} \text{Tr} \left(\bar{\mathbf{U}}_k \mathbf{Y}_k^H \sum_{l=1}^{\mathcal{L}} \sum_{i=1}^{\mathcal{K}} \bar{\mathbf{D}}_{l,k}^H \mathbf{W}_{l,i} \mathbf{W}_{l,i}^H \bar{\mathbf{D}}_{l,k} \mathbf{Y}_k \right) \right\}}_{(a)} \\
&+ \underbrace{\mathbb{E} \left\{ \sum_{k=1}^{\mathcal{K}} \text{Tr} \left(\bar{\mathbf{U}}_k \mathbf{Y}_k^H \sum_{l=1}^{\mathcal{L}} \sum_{i=1}^{\mathcal{K}} \bar{\mathbf{G}}_k^H \boldsymbol{\Theta} \hat{\mathbf{S}}_l \mathbf{W}_{l,i} \mathbf{W}_{l,i}^H \hat{\mathbf{S}}_l^H \boldsymbol{\Theta}^H \bar{\mathbf{G}}_k \mathbf{Y}_k \right) \right\}}_{(b)} \\
&+ \underbrace{\mathbb{E} \left\{ \sum_{k=1}^{\mathcal{K}} \text{Tr} \left(\bar{\mathbf{U}}_k \mathbf{Y}_k^H \sum_{l=1}^{\mathcal{L}} \sum_{i=1}^{\mathcal{K}} \hat{\mathbf{G}}_k^H \boldsymbol{\Theta} \bar{\mathbf{S}}_l \mathbf{W}_{l,i} \mathbf{W}_{l,i}^H \bar{\mathbf{S}}_l^H \boldsymbol{\Theta}^H \hat{\mathbf{G}}_k \mathbf{Y}_k \right) \right\}}_{(c)} \\
&+ \underbrace{\mathbb{E} \left\{ \sum_{k=1}^{\mathcal{K}} \text{Tr} \left(\bar{\mathbf{U}}_k \mathbf{Y}_k^H \sum_{l=1}^{\mathcal{L}} \sum_{i=1}^{\mathcal{K}} \bar{\mathbf{G}}_k^H \boldsymbol{\Theta} \bar{\mathbf{S}}_l \mathbf{W}_{l,i} \mathbf{W}_{l,i}^H \bar{\mathbf{S}}_l^H \boldsymbol{\Theta}^H \bar{\mathbf{G}}_k \mathbf{Y}_k \right) \right\}}_{(d)}. \tag{44}
\end{aligned}$$

The above equation holds based on the fact that $\mathbb{E} \{ \bar{\mathbf{S}}_{l,r} \} = \mathbb{E} \{ \bar{\mathbf{G}}_{r,k} \} = \mathbb{E} \{ \bar{\mathbf{D}}_{l,k} \} = \mathbf{0}, \forall l, r, k$.

In order to complete this proof, we make use of the following properties for any matrices of appropriate dimensions:

$$\text{Tr}(\mathbf{A}^T \mathbf{B}) = \text{Vec}(\mathbf{A})^T \text{Vec}(\mathbf{B}), \tag{45a}$$

$$\text{Tr}(\mathbf{A} \otimes \mathbf{B}) = \text{Tr}(\mathbf{A}) \text{Tr}(\mathbf{B}), \tag{45b}$$

$$\text{Vec}(\mathbf{ABC}) = (\mathbf{C}^T \otimes \mathbf{A}) \text{Vec}(\mathbf{B}), \tag{45c}$$

$$\text{Tr}(\mathbf{AMB}) = \mathbf{m}^T (\mathbf{A} \odot \mathbf{B}) \mathbf{m}, \tag{45d}$$

$$\mathbf{A} \odot \mathbf{I} = \text{Diag}(\mathbf{A}_{1,1}, \mathbf{A}_{2,2}, \dots, \mathbf{A}_{J,J}), \tag{45e}$$

$$\mathbb{E} \{ \mathbf{x}^T \mathbf{A} \mathbf{x} \} = \text{Tr}(\mathbf{A} \boldsymbol{\Sigma}) + \mathbf{c}^T \mathbf{A} \mathbf{c}, \tag{45f}$$

where $\mathbf{M} = \text{Diag}(\mathbf{m})$ and $\mathbf{m} = \text{Vecd}(\mathbf{M})$, and \mathbf{x} is a stochastic vector with mean \mathbf{c} and covariance $\boldsymbol{\Sigma}$. The proofs of above matrix manipulations can be found in [45] and [42].

Then, in the following, we analysis the expectation terms (a), (b), (c), (d), respectively. First, we can express the expected value of the term (a) as

$$(a) = \mathbb{E} \left\{ \sum_{k=1}^{\mathcal{K}} \sum_{l=1}^{\mathcal{L}} \sum_{i=1}^{\mathcal{K}} \text{Vec}(\bar{\mathbf{D}}_{l,k})^H \text{Vec}(\mathbf{W}_{l,i} \mathbf{W}_{l,i}^H \bar{\mathbf{D}}_{l,k} \mathbf{Y}_k \bar{\mathbf{U}}_k \mathbf{Y}_k^H) \right\} \quad (46a)$$

$$= \mathbb{E} \left\{ \sum_{k=1}^{\mathcal{K}} \sum_{l=1}^{\mathcal{L}} \sum_{i=1}^{\mathcal{K}} \text{Vec}(\bar{\mathbf{D}}_{l,k})^H \left((\mathbf{Y}_k \bar{\mathbf{U}}_k \mathbf{Y}_k^H)^T \otimes (\mathbf{W}_{l,i} \mathbf{W}_{l,i}^H) \right) \text{Vec}(\bar{\mathbf{D}}_{l,k}) \right\} \quad (46b)$$

$$= \sum_{k=1}^{\mathcal{K}} \sum_{l=1}^{\mathcal{L}} \sum_{i=1}^{\mathcal{K}} \delta_{\mathbf{D}_{l,k}}^2 \text{Tr} \left((\mathbf{Y}_k \bar{\mathbf{U}}_k \mathbf{Y}_k^H)^T \otimes (\mathbf{W}_{l,i} \mathbf{W}_{l,i}^H) \right) \quad (46c)$$

$$= \sum_{k=1}^{\mathcal{K}} \sum_{l=1}^{\mathcal{L}} \sum_{i=1}^{\mathcal{K}} \delta_{\mathbf{D}_{l,k}}^2 \text{Tr}(\mathbf{Y}_k \bar{\mathbf{U}}_k \mathbf{Y}_k^H) \text{Tr}(\mathbf{W}_{l,i} \mathbf{W}_{l,i}^H), \quad (46d)$$

where (46a), (46b), (46c), (46d) can be achieved by employing the properties (45a), (45c), (45f), (45b), respectively.

Then, we can express the expected value of the term (b) as

$$(b) = \sum_{k=1}^{\mathcal{K}} \sum_{l=1}^{\mathcal{L}} \sum_{i=1}^{\mathcal{K}} \delta_{\mathbf{G}_k}^2 \text{Tr}(\mathbf{Y}_k \bar{\mathbf{U}}_k \mathbf{Y}_k^H) \text{Tr}(\Theta \hat{\mathbf{S}}_l \mathbf{W}_{l,i} \mathbf{W}_{l,i}^H \hat{\mathbf{S}}_l^H \Theta^H) \quad (47a)$$

$$= \sum_{k=1}^{\mathcal{K}} \sum_{l=1}^{\mathcal{L}} \sum_{i=1}^{\mathcal{K}} \alpha^2 \delta_{\mathbf{G}_k}^2 \text{Tr}(\mathbf{Y}_k \bar{\mathbf{U}}_k \mathbf{Y}_k^H) \text{Tr}(\hat{\mathbf{S}}_l \mathbf{W}_{l,i} \mathbf{W}_{l,i}^H \hat{\mathbf{S}}_l^H), \quad (47b)$$

where the proof of (47a) is the same as (46), and (47a) holds based on the property of the trace operator, i.e., $\text{Tr}(\mathbf{ABC}) = \text{Tr}(\mathbf{BCA}) = \text{Tr}(\mathbf{CAB})$ and $\Theta^H \Theta = \alpha^2 \mathbf{I}_{\mathcal{RN}}$. Besides, (47b) can also be proved by employing (45d) and (45e) as follows:

$$\text{Tr}(\Theta \hat{\mathbf{S}}_l \mathbf{W}_{l,i} \mathbf{W}_{l,i}^H \hat{\mathbf{S}}_l^H \Theta) = \text{Vecd}(\Theta)^H \left(\mathbf{I} \odot (\hat{\mathbf{S}}_l \mathbf{W}_{l,i} \mathbf{W}_{l,i}^H \hat{\mathbf{S}}_l^H) \right) \text{Vecd}(\Theta) \quad (48a)$$

$$= \text{Vecd}(\Theta)^H \text{Diag}(\hat{\mathbf{S}}_l \mathbf{W}_{l,i} \mathbf{W}_{l,i}^H \hat{\mathbf{S}}_l^H) \text{Vecd}(\Theta) \quad (48b)$$

$$= \alpha^2 \text{Tr}(\hat{\mathbf{S}}_l \mathbf{W}_{l,i} \mathbf{W}_{l,i}^H \hat{\mathbf{S}}_l^H), \quad (48c)$$

where (48c) holds based on the definition of the trace operator and $\Theta_{n,n}^* \Theta_{n,n} = \alpha^2, \forall n$.

Similarly, the expected value of the term (c) can be expressed as

$$(c) = \sum_{k=1}^{\mathcal{K}} \sum_{l=1}^{\mathcal{L}} \sum_{i=1}^{\mathcal{K}} \alpha^2 \delta_{\mathbf{S}_l}^2 \text{Tr}(\hat{\mathbf{G}}_k \mathbf{Y}_k \bar{\mathbf{U}}_k \mathbf{Y}_k^H \hat{\mathbf{G}}_k^H) \text{Tr}(\mathbf{W}_{l,i} \mathbf{W}_{l,i}^H). \quad (49)$$

Further, the expected value of the term (d) can be determined by

$$(d) = \sum_{k=1}^{\mathcal{K}} \sum_{l=1}^{\mathcal{L}} \sum_{i=1}^{\mathcal{K}} \alpha^2 \delta_{\mathbf{G}_k}^2 \text{Tr}(\mathbf{Y}_k \bar{\mathbf{U}}_k \mathbf{Y}_k^H) \text{Tr}(\bar{\mathbf{S}}_l \mathbf{W}_{l,i} \mathbf{W}_{l,i}^H \bar{\mathbf{S}}_l^H) \quad (50a)$$

$$= \sum_{k=1}^{\mathcal{K}} \sum_{l=1}^{\mathcal{L}} \sum_{i=1}^{\mathcal{K}} \alpha^2 \delta_{\mathbf{S}_l}^2 \delta_{\mathbf{G}_k}^2 \text{Tr}(\mathbf{Y}_k \bar{\mathbf{U}}_k \mathbf{Y}_k^H) \text{Tr}(\mathbf{W}_{l,i} \mathbf{W}_{l,i}^H \otimes \mathbf{I}_{\mathcal{RN}}) \quad (50b)$$

$$= \sum_{k=1}^{\mathcal{K}} \sum_{l=1}^{\mathcal{L}} \sum_{i=1}^{\mathcal{K}} \mathcal{RN} \alpha^2 \delta_{\mathbf{S}_l}^2 \delta_{\mathbf{G}_k}^2 \text{Tr}(\mathbf{Y}_k \bar{\mathbf{U}}_k \mathbf{Y}_k^H) \text{Tr}(\mathbf{W}_{l,i} \mathbf{W}_{l,i}^H), \quad (50c)$$

where (50b) and (50c) hold based on (45f) and $\text{Tr}(\mathbf{I}_{\mathcal{RN}}) = \mathcal{RN}$, respectively.

Thus, the transformations given above verify that the expectation term in (44) with respect to CSI uncertainties has no direct impact on the optimizing of the passive reflecting beamforming. This completes the proof of Proposition 2.

B. Proof of Lemma 1

Let ρ_i^{u+1} denote the value of the objective function of ρ^{u+1} after updating the i -th element and fixing the others $\tilde{\mathcal{N}} - 1$ elements of $\boldsymbol{\theta}$ in u -th sub-iteration, we have

$$\rho^u \leq \rho_1^{u+1} \leq \rho_2^{u+1} \cdots \leq \rho_{\tilde{\mathcal{N}}}^{u+1} = \rho^{u+1}, \quad (51)$$

which shows that the value of the objective function in the problem $\mathcal{P}5$ achieved by Algorithm 2 increases monotonically. Meanwhile, we have

$$-\boldsymbol{\theta}^H \mathbf{Z} \boldsymbol{\theta} \leq -\alpha^2 \tilde{\mathcal{N}} \lambda_{\mathbf{Z}}^{\min}, \quad (52a)$$

$$\text{Re} \{ \boldsymbol{\theta}^H \boldsymbol{\omega} \} \leq \alpha \sum_{n=1}^{\tilde{\mathcal{N}}} |\boldsymbol{\omega}_n|, \quad (52b)$$

where $\lambda_{\mathbf{Z}}^{\min}$ is the minimum eigenvalue of \mathbf{Z} . The above inequalities yield that the optimal objective value is upper-bounded by a finite value. Therefore, Algorithm 2 is guaranteed to converge. This completes the proof of Lemma 1.

REFERENCES

- [1] D. Gesbert, S. Hanly, H. Huang, S. Shama Shitz, O. Simeone, and W. Yu, "Multi-Cell MIMO Cooperative Networks: A New Look at Interference," *IEEE Journal on Selected Areas in Communications*, vol. 28, no. 9, pp. 1380–1408, 2010.
- [2] E. Nayeri, A. Ashikhmin, T. L. Marzetta, H. Yang, and B. D. Rao, "Precoding and Power Optimization in Cell-Free Massive MIMO Systems," *IEEE Transactions on Wireless Communications*, vol. 16, no. 7, pp. 4445–4459, 2017.
- [3] L. Du, L. Li, H. Q. Ngo, T. C. Mai, and M. Matthaiou, "Cell-Free Massive MIMO: Joint Maximum-Ratio and Zero-Forcing Precoder With Power Control," *IEEE Transactions on Communications*, vol. 69, no. 6, pp. 3741–3756, 2021.
- [4] H. Q. Ngo, A. Ashikhmin, H. Yang, E. G. Larsson, and T. L. Marzetta, "Cell-Free Massive MIMO Versus Small Cells," *IEEE Transactions on Wireless Communications*, vol. 16, no. 3, pp. 1834–1850, 2017.
- [5] X. Hu, C. Zhong, Y. Zhu, X. Chen, and Z. Zhang, "Programmable Metasurface-Based Multicast Systems: Design and Analysis," *IEEE Journal on Selected Areas in Communications*, vol. 38, no. 8, pp. 1763–1776, 2020.
- [6] M. Di Renzo, A. Zappone, M. Debbah, M. S. Alouini, C. Yuen, J. de Rosny, and S. Tretakov, "Smart Radio Environments Empowered by Reconfigurable Intelligent Surfaces: How It Works, State of Research, and The Road Ahead," *IEEE Journal on Selected Areas in Communications*, vol. 38, no. 11, pp. 2450–2525, 2020.
- [7] M. Di Renzo, M. Debbah, D.-T. Phan-Huy, A. Zappone, M.-S. Alouini, C. Yuen, V. Sciancalepore, G. C. Alexandropoulos, J. Hoydis, H. Gacanin, *et al.*, "Smart radio environments empowered by reconfigurable AI meta-surfaces: An idea whose time has come," *EURASIP Journal on Wireless Communications and Networking*, vol. 2019, no. 1, pp. 1–20, 2019.

- [8] H. Guo, Y. Liang, J. Chen, and E. G. Larsson, "Weighted Sum-Rate Maximization for Reconfigurable Intelligent Surface Aided Wireless Networks," *IEEE Transactions on Wireless Communications*, vol. 19, no. 5, pp. 3064–3076, 2020.
- [9] M. A. Saeidi, M. J. Emadi, H. Masoumi, M. R. Mili, D. W. K. Ng, and I. Krikidis, "Weighted Sum-Rate Maximization for Multi-IRS-Assisted Full-Duplex Systems With Hardware Impairments," *IEEE Transactions on Cognitive Communications and Networking*, vol. 7, no. 2, pp. 466–481, 2021.
- [10] C. Pan, H. Ren, K. Wang, W. Xu, M. ElKashlan, A. Nallanathan, and L. Hanzo, "Multicell MIMO Communications Relying on Intelligent Reflecting Surfaces," *IEEE Transactions on Wireless Communications*, vol. 19, no. 8, pp. 5218–5233, 2020.
- [11] S. Zhang and R. Zhang, "Capacity Characterization for Intelligent Reflecting Surface Aided MIMO Communication," *IEEE Journal on Selected Areas in Communications*, vol. 38, no. 8, pp. 1823–1838, 2020.
- [12] Q. Wu and R. Zhang, "Beamforming Optimization for Wireless Network Aided by Intelligent Reflecting Surface With Discrete Phase Shifts," *IEEE Transactions on Communications*, vol. 68, no. 3, pp. 1838–1851, 2020.
- [13] L. You, J. Xiong, Y. Huang, D. W. K. Ng, C. Pan, W. Wang, and X. Gao, "Reconfigurable Intelligent Surfaces-Assisted Multiuser MIMO Uplink Transmission With Partial CSI," *IEEE Transactions on Wireless Communications*, vol. 20, no. 9, pp. 5613–5627, 2021.
- [14] M. Hua, Q. Wu, D. W. K. Ng, J. Zhao, and L. Yang, "Intelligent Reflecting Surface-Aided Joint Processing Coordinated Multipoint Transmission," *IEEE Transactions on Communications*, vol. 69, no. 3, pp. 1650–1665, 2021.
- [15] Y. Zhang, B. Di, H. Zhang, J. Lin, C. Xu, D. Zhang, Y. Li, and L. Song, "Beyond Cell-Free MIMO: Energy Efficient Reconfigurable Intelligent Surface Aided Cell-Free MIMO Communications," *IEEE Transactions on Cognitive Communications and Networking*, vol. 7, no. 2, pp. 412–426, 2021.
- [16] Z. Zhang and L. Dai, "A Joint Precoding Framework for Wideband Reconfigurable Intelligent Surface-Aided Cell-Free Network," *IEEE Transactions on Signal Processing*, pp. 1–1, 2021.
- [17] G. Zhou, C. Pan, H. Ren, K. Wang, and A. Nallanathan, "A Framework of Robust Transmission Design for IRS-Aided MISO Communications With Imperfect Cascaded Channels," *IEEE Transactions on Signal Processing*, vol. 68, pp. 5092–5106, 2020.
- [18] Z. Zhou, N. Ge, Z. Wang, and L. Hanzo, "Joint Transmit Precoding and Reconfigurable Intelligent Surface Phase Adjustment: A Decomposition-Aided Channel Estimation Approach," *IEEE Transactions on Communications*, vol. 69, no. 2, pp. 1228–1243, 2021.
- [19] Z. Wang, L. Liu, and S. Cui, "Channel Estimation for Intelligent Reflecting Surface Assisted Multiuser Communications: Framework, Algorithms, and Analysis," *IEEE Transactions on Wireless Communications*, vol. 19, no. 10, pp. 6607–6620, 2020.
- [20] K. Ardah, S. Gharekhloo, A. L. F. de Almeida, and M. Haardt, "TRICE: A Channel Estimation Framework for RIS-Aided Millimeter-Wave MIMO Systems," *IEEE Signal Processing Letters*, vol. 28, pp. 513–517, 2021.
- [21] L. Wei, C. Huang, G. C. Alexandropoulos, C. Yuen, Z. Zhang, and M. Debbah, "Channel Estimation for RIS-Empowered Multi-User MISO Wireless Communications," *IEEE Transactions on Communications*, vol. 69, no. 6, pp. 4144–4157, 2021.
- [22] P. Ubaidulla and A. Chockalingam, "Relay Precoder Optimization in MIMO-Relay Networks With Imperfect CSI," *IEEE Transactions on Signal Processing*, vol. 59, no. 11, pp. 5473–5484, 2011.
- [23] S. Zargari, S. Farahmand, B. Abolhassani, and C. Tellambura, "Robust Active and Passive Beamformer Design for IRS-Aided Downlink MISO PS-SWIPT With a Nonlinear Energy Harvesting Model," *IEEE Transactions on Green Communications and Networking*, vol. 5, no. 4, pp. 2027–2041, 2021.
- [24] Z. Zhang, L. Lv, Q. Wu, H. Deng, and J. Chen, "Robust and Secure Communications in Intelligent Reflecting Surface Assisted NOMA Networks," *IEEE Communications Letters*, vol. 25, no. 3, pp. 739–743, 2021.

- [25] X. Yu, D. Xu, Y. Sun, D. W. K. Ng, and R. Schober, "Robust and Secure Wireless Communications via Intelligent Reflecting Surfaces," *IEEE Journal on Selected Areas in Communications*, vol. 38, no. 11, pp. 2637–2652, 2020.
- [26] H.-H. Lee, Y.-C. Ko, and H.-C. Yang, "On Robust Weighted Sum Rate Maximization for MIMO Interfering Broadcast Channels with Imperfect Channel Knowledge," *IEEE Communications Letters*, vol. 17, no. 6, pp. 1156–1159, 2013.
- [27] S. Hong, C. Pan, H. Ren, K. Wang, K. K. Chai, and A. Nallanathan, "Robust Transmission Design for Intelligent Reflecting Surface-Aided Secure Communication Systems With Imperfect Cascaded CSI," *IEEE Transactions on Wireless Communications*, vol. 20, no. 4, pp. 2487–2501, 2021.
- [28] H. Niu, Z. Chu, F. Zhou, Z. Zhu, L. Zhen, and K.-K. Wong, "Robust Design for Intelligent Reflecting Surface Assisted Secrecy SWIPT Network," *IEEE Transactions on Wireless Communications*, pp. 1–1, 2021.
- [29] Y. Jia, Y. Cui, and W. Jiang, "Robust Optimization of Instantaneous Beamforming and Quasi-static Phase Shifts in an IRS-assisted Multi-Cell Network," *IEEE Transactions on Wireless Communications*, pp. 1–1, 2021.
- [30] J. Zhang, Y. Zhang, C. Zhong, and Z. Zhang, "Robust Design for Intelligent Reflecting Surfaces Assisted MISO Systems," *IEEE Communications Letters*, vol. 24, no. 10, pp. 2353–2357, 2020.
- [31] Y. Omid, S. M. Shahabi, C. Pan, Y. Deng, and A. Nallanathan, "Low-Complexity Robust Beamforming Design for IRS-Aided MISO Systems With Imperfect Channels," *IEEE Communications Letters*, vol. 25, no. 5, pp. 1697–1701, 2021.
- [32] S. Zhang and R. Zhang, "Intelligent Reflecting Surface Aided Multi-User Communication: Capacity Region and Deployment Strategy," *IEEE Transactions on Communications*, vol. 69, no. 9, pp. 5790–5806, 2021.
- [33] Q. Wu and R. Zhang, "Joint Active and Passive Beamforming Optimization for Intelligent Reflecting Surface Assisted SWIPT Under QoS Constraints," *IEEE Journal on Selected Areas in Communications*, vol. 38, no. 8, pp. 1735–1748, 2020.
- [34] S. Zargari, A. Khalili, Q. Wu, M. Robat Mili, and D. W. K. Ng, "Max-Min Fair Energy-Efficient Beamforming Design for Intelligent Reflecting Surface-Aided SWIPT Systems With Non-Linear Energy Harvesting Model," *IEEE Transactions on Vehicular Technology*, vol. 70, no. 6, pp. 5848–5864, 2021.
- [35] Q. Wu, S. Zhang, B. Zheng, C. You, and R. Zhang, "Intelligent Reflecting Surface-Aided Wireless Communications: A Tutorial," *IEEE Transactions on Communications*, vol. 69, no. 5, pp. 3313–3351, 2021.
- [36] K. Shen and W. Yu, "Fractional programming for communication systems—Part II: Uplink scheduling via matching," *IEEE Transactions on Signal Processing*, vol. 66, no. 10, pp. 2631–2644, 2018.
- [37] K. Shen and W. Yu, "Fractional programming for communication systems—Part I: Power control and beamforming," *IEEE Transactions on Signal Processing*, vol. 66, no. 10, pp. 2616–2630, 2018.
- [38] Q. Shi, M. Razaviyayn, Z. Luo, and C. He, "An Iteratively Weighted MMSE Approach to Distributed Sum-Utility Maximization for a MIMO Interfering Broadcast Channel," *IEEE Transactions on Signal Processing*, vol. 59, no. 9, pp. 4331–4340, 2011.
- [39] M. Grant and S. Boyd, "CVX: Matlab Software for Disciplined Convex Programming, version 2.1." <http://cvxr.com/cvx>, Mar. 2014.
- [40] S. Boyd, S. P. Boyd, and L. Vandenberghe, *Convex optimization*. Cambridge university press, 2004.
- [41] H.-J. Choi, K.-J. Lee, C. Song, H. Song, and I. Lee, "Weighted Sum Rate Maximization for Multiuser Multirelay MIMO Systems," *IEEE Transactions on Vehicular Technology*, vol. 62, no. 2, pp. 885–889, 2013.
- [42] X. Zhang, *Matrix Analysis and Applications*. Cambridge University Press, 2017.
- [43] G. Cui, X. Yu, G. Foglia, Y. Huang, and J. Li, "Quadratic Optimization With Similarity Constraint for Unimodular Sequence Synthesis," *IEEE Transactions on Signal Processing*, vol. 65, no. 18, pp. 4756–4769, 2017.
- [44] H. Li, W. Cai, Y. Liu, M. Li, Q. Liu, and Q. Wu, "Intelligent Reflecting Surface Enhanced Wideband MIMO-OFDM

Communications: From Practical Model to Reflection Optimization,” *IEEE Transactions on Communications*, vol. 69, no. 7, pp. 4807–4820, 2021.

[45] K. B. Petersen and M. S. Pedersen, “The matrix cookbook,” nov 2012. Version 20121115.